



**HAL**  
open science

# Superimposed Rifting at the Junction of the Central and Equatorial Atlantic: Formation of the Passive Margin of the Guiana Shield

Artiom Loparev, Delphine Rouby, Dominique Chardon, Massimo Dall'asta,  
François Sapin, Flora Bajolet, Jing Ye, Fabien Paquet

## ► To cite this version:

Artiom Loparev, Delphine Rouby, Dominique Chardon, Massimo Dall'asta, François Sapin, et al.. Superimposed Rifting at the Junction of the Central and Equatorial Atlantic: Formation of the Passive Margin of the Guiana Shield. *Tectonics*, 2021, 40 (7), 10.1029/2020TC006159 . insu-03341865

**HAL Id: insu-03341865**

**<https://insu.hal.science/insu-03341865>**

Submitted on 13 Sep 2021

**HAL** is a multi-disciplinary open access archive for the deposit and dissemination of scientific research documents, whether they are published or not. The documents may come from teaching and research institutions in France or abroad, or from public or private research centers.

L'archive ouverte pluridisciplinaire **HAL**, est destinée au dépôt et à la diffusion de documents scientifiques de niveau recherche, publiés ou non, émanant des établissements d'enseignement et de recherche français ou étrangers, des laboratoires publics ou privés.



Distributed under a Creative Commons Attribution - ShareAlike 4.0 International License

# Tectonics

## RESEARCH ARTICLE

10.1029/2020TC006159

### Key Points:

- Higher rifting obliquity and rates produced narrower rift and rifted margin segments
- Warmer Central Atlantic rifting produced crustal flow and preserved thick syn-rift deposits contrary to cooler Equatorial Atlantic rifting
- Lithosphere of the Demerara Plateau was thinned twice and became a buoyant continental raft since the Mid-Cretaceous

### Supporting Information:

Supporting Information may be found in the online version of this article.

### Correspondence to:

D. Rouby,  
Delphine.Rouby@get.omp.eu

### Citation:

Loparev, A., Rouby, D., Chardon, D., Dall'Asta, M., Sapin, F., Bajolet, F., et al. (2021). Superimposed rifting at the junction of the Central and Equatorial Atlantic: Formation of the passive margin of the Guiana Shield. *Tectonics*, 40, e2020TC006159. <https://doi.org/10.1029/2020TC006159>

Received 25 FEB 2020  
Accepted 4 JUN 2021

© 2021. The Authors.

This is an open access article under the terms of the [Creative Commons Attribution-NonCommercial License](#), which permits use, distribution and reproduction in any medium, provided the original work is properly cited and is not used for commercial purposes.

# Superimposed Rifting at the Junction of the Central and Equatorial Atlantic: Formation of the Passive Margin of the Guiana Shield

Artiom Loparev<sup>1</sup>, Delphine Rouby<sup>1</sup> , Dominique Chardon<sup>1</sup> , Massimo Dall'Asta<sup>2</sup>, François Sapin<sup>2</sup>, Flora Bajolet<sup>1,3</sup>, Jing Ye<sup>1</sup>, and Fabien Paquet<sup>3</sup>

<sup>1</sup>GET, Université de Toulouse, CNRS, IRD, UPS, CNES, Toulouse, France, <sup>2</sup>TOTAL, Centre Scientifique et Technique Jean Féger, Pau, France, <sup>3</sup>BRGM, Orléans, France

**Abstract** The passive margin of the Guiana Shield formed at the junction of the Central and Equatorial Atlantic Oceans that developed successively by a complex rifting process that achieved the final dispersal of Western Gondwana. Yet, the resulting spatial distribution of crustal thinning along the margin remains to be mapped and its controlling parameters deciphered. We used subsurface data to map the variability of crustal thinning along the margin. We show that the margin segments width primarily depends on their obliquity to rifting extension direction. The necking domain of the transform/oblique margin segments is much narrower (<100 km) than divergent segments that include hyper-extended or distal margin domains as well (200–300 km). Moreover, for a similar obliquity, the width of margin segments resulting from the Central Atlantic rifting are wider than those resulting from the Equatorial Atlantic rifting. This is primarily due to the higher obliquity and rate of the latter. Additionally, along the Central Atlantic margin segments, thinning was accommodated by lower-crustal ductile deformation, the thick syn-rift in-fill was associated with magmatism and a thicker than average oceanic crust. In contrast, the Equatorial Atlantic margin segments show little ductile deformation, reduced clastic syn-rift infill and thinner than average oceanic crust. These observations suggest that the lithosphere affected by the Central Atlantic rifting was warmer than that affected by the Equatorial Atlantic rifting. Finally, the two-step thinning in the overlapping area of the two rift systems individualized a promontory of thinned continental crust that remained as the Demerara Plateau.

**Plain Language Summary** The continental margin of the Guiana Shield formed at the intersection of the Central and Equatorial Atlantic Oceans that developed one after the other and, in doing so, achieved the break-up of the Gondwana supercontinent. To form these Ocean, the continent crust was stretched and broke but the way this thinning is actually varying along the margin and the causes are not known so we used offshore industrial data to map it. This allows us showing that the width of the continental margin depends primarily on the direction along which the crust was thinned such that the continental margin width is much wider (200–300 km) in domains where this direction is perpendicular to the margin than in domain where it is oblique (<100 km). This also allow us showing that the continental margin resulting from the opening of the Central Atlantic Ocean is systematically wider than the one resulting from the opening of the Equatorial Atlantic. Additionally, our observations suggest that Central Atlantic Ocean opened under warmer conditions than the Equatorial Atlantic. Finally, the area at the intersection of the Central and Equatorial Atlantic Oceans, individualized a promontory of continental crust that formed the present-day Demerara Plateau.

## 1. Introduction

Continental break-up is often accommodated by complex three-dimensional (3D) rifting patterns at continental scale (e.g., Frizon de Lamotte et al., 2015; Merdith et al., 2019; Stampfli & Borel, 2002). For example, the dispersal of Western Gondwana generated several successive and locally overlapping oblique rifts across the African and South American plates such as the West and Central African Rift Systems (e.g., Fairhead, 1988; Genik, 1992; Guiraud et al., 1992), East African Rift (Morley et al., 1992; Versfelt & Rosen-dahl, 1989) or the Equatorial Atlantic rift (e.g., Basile et al., 2005; Mascle & Blarez, 1987).

Such riftings are expected to produce complex 3D deformation patterns whose impact on the spatial partitioning of crustal thinning at continental scale has however not been fully explored yet. Many studies have concentrated on the influence of lithosphere rheology, rifting rates and obliquity on the geometry of rifts and resulting rifted margins. For example, higher deformation rates or higher extension obliquity produce narrower rifts and rifted margins as shown from either global compilation (e.g., Jeannot & Buitter, 2018), continental scale studies (e.g., Ye et al., 2019) or modeling (Brune, 2014; Buck, 1991; Clifton et al., 2000; Svartman Dias et al., 2015; Tetreault & Buitter, 2018; Tron & Brun, 1991). Other studies have related the segmentation of rifted margins to the structural inheritance of the continental basement in natural systems (e.g., Bellahsen et al., 2013; Schiffer et al., 2020; Stanton et al., 2019) or experiments (e.g., Autin et al., 2013; Duclaux et al., 2020). However, the spatial variation at continental scale in the width of a rift that underwent both oblique extension and the superimposition of rifting episodes has not been documented in natural systems yet. This is however of primary importance to understand how crustal thinning is distributed in three-dimensions during continental break-up, with implications on the crustal and stratigraphic architectures of the resulting rifted margins.

The Equatorial Atlantic rifting achieved the final dispersal of Western Gondwana by connecting the Central Atlantic Ocean, formed in the Jurassic (ca. 190 Ma onward), to the South Atlantic Ocean, formed in the Cretaceous (ca. 135 Ma onward; e.g., Heine et al., 2013; Labails et al., 2010; Moulin et al., 2010; Ye et al., 2017). The mid-Cretaceous opening of the Equatorial Atlantic Ocean (since ca. 130 Ma) led to a remarkable example of oblique and superimposed rifting pattern (e.g., Benkhelil et al., 1995; Ye et al., 2017). This rifting resulted from continental scale right-lateral shearing between South America and Africa and formed an en-échelon rift system (e.g., Benkhelil et al., 1995; Guiraud et al., 1992; Mascle et al., 1988; Ye et al., 2017). It produced a complex 3D lithospheric and crustal stretching pattern (e.g., Kuszniir et al., 2018; Ye et al., 2019). Benkhelil et al. (1995), Mercier de Lépinay (2016) and Ye et al. (2017) showed that the Equatorial Atlantic Rift (EAR) partly propagated through crustal domains that had previously undergone thinning during formation of the Central Atlantic Rift (CAR). Moreover, the two rift systems had contrasted opening modes: the CAR system had lower obliquity (extension direction at a high angle to the margin trend) and velocity than the EAR (Brune et al., 2016, 2018). The CAR developed contemporaneously with magmatism (Basile et al., 2020; Museur et al., 2020; Nemčok et al., 2016; Reuber et al., 2016), which is not the case for the EAR (e.g., Greenroyd et al., 2008; Loncke et al., 2009).

The mid-Cretaceous (ca. 130–100 Ma) rifting of the Equatorial Atlantic Ocean is therefore a relevant case study to investigate the spatial evolution of deformation and necking styles (i.e., crustal architecture, brittle/ductile strain partitioning, and syn-rift fault vergence) along segmented conjugated margins that underwent both oblique extension and rifts superimposition. Previous geological studies of the Equatorial Atlantic rift have mostly investigated the development of individual basins along the African rifted margin (e.g., Antobreh et al., 2009; Basile et al., 1998; Olyphant et al., 2017; Scarselli et al., 2018) or its conjugate south American counterpart (e.g., Loncke et al., 2016; Sapin et al., 2016; Yang & Escalona, 2011). Kuszniir et al. (2018) documented, at continental scale, the variability of the crustal structure along both margins of the Equatorial Atlantic. Ye et al. (2019) have shown that the necking width of the African margin segments depended primarily on their obliquity to extension direction. However, no comparable synthesis is available for the South American conjugate margin of the Equatorial Atlantic.

In this work, we investigate the influence of the kinematics and the superimposition of the CAR and EAR on the first-order geometry of the resulting South American passive margin along the Guiana Shield (i.e., including the Guiana-Surinam and Foz do Amazonas basins separated by the Demerara plateau; Figure 1). To do this, we used an extensive set of subsurface data (two-dimensional [2D] seismic and wells provided by Total). We characterize the variability of crustal architecture and thinning processes along the margin and integrate the distribution of the crustal thinning within a consistent plate-scale kinematics framework.

## 2. Geological and Geodynamical Settings

### 2.1. The Guiana Shield Passive Margin

The passive margin of the Guiana Shield is located between, to the NW, the Barbados accretionary prism forming the Caribbean subduction front (Pindell & Kennan, 2009; Yang & Escalona, 2011) and, to the SE,

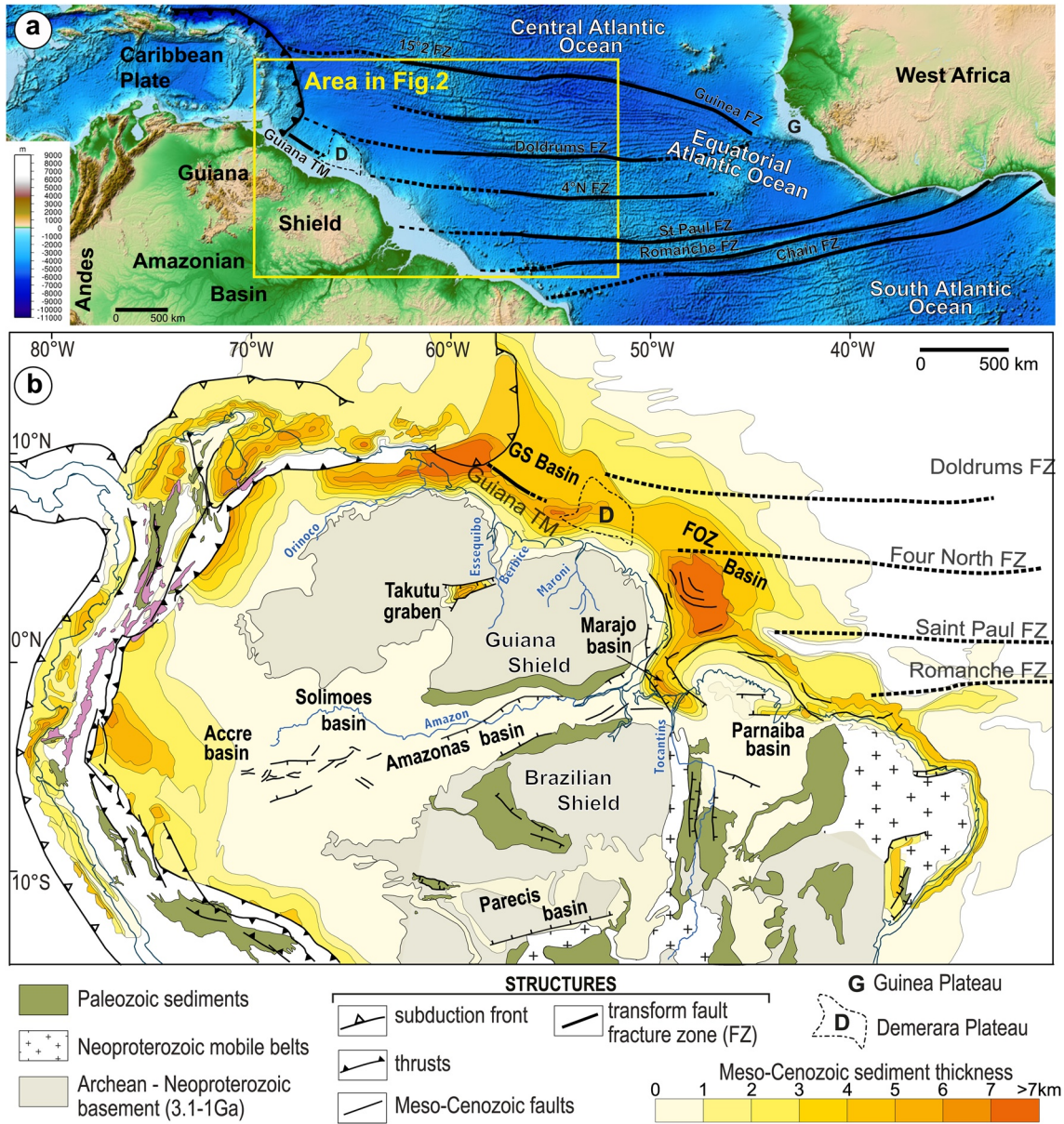


**Figure 1.** (a) Location of the study area. (b) Simplified geological map of northern South America showing the context of the Guiana Shield and its margin with Mesozoic-Cenozoic sediments thickness (modified after Cordani et al., 2016). FOZ, Foz d'Amazonas; FZ, transform fracture zone; GS, Guiana-Suriname; TM, transform margin. Topography and bathymetry after NOAA (2009).

by the Saint Paul Fracture Zone (FZ; Cordani et al., 2016, Figures 1 and 2). The northwestern portion of the margin, that is, between the Caribbean subduction and the Demerara Plateau, is floored by Jurassic oceanic crust accreted following rifting of the Central Atlantic Ocean (Klitgord & Schouten, 1986; Pindell, 1985; Reuber et al., 2016; Figure 2). That portion of the margin coincides with the Guiana-Suriname basin, called hereafter the GS basin. The remaining southeastern portion of the margin is floored by Cretaceous oceanic crust formed following rifting of the Equatorial Atlantic Ocean (Heine et al., 2013; Moulin et al., 2010; Figures 1 and 2). That portion of the margin coincides with the northern and eastern Demerara Plateau and Foz de Amazonas basin, called hereafter the FOZ basin.

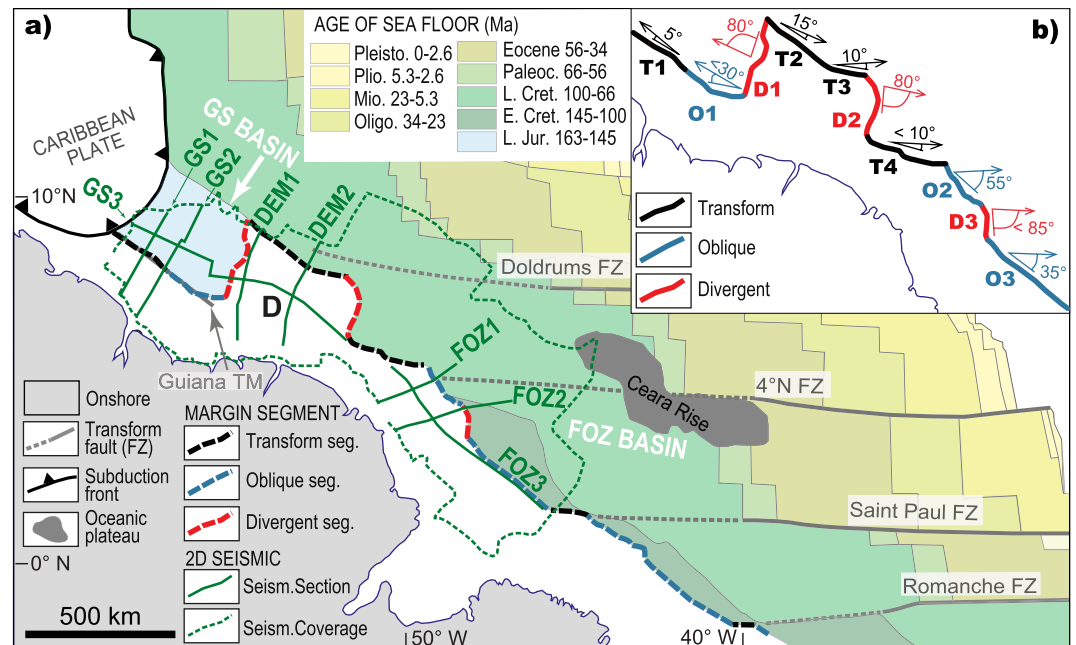


**Figure 2.** (a) Location of the geological sections of Figures 4 to 6 (in green), as well as the areal extent of the studied subsurface database (2D seismic and well logs; green dashed line). Oceanic geology adapted from Cordani et al. (2016). The frame of the map area is located on Figure 1a. (b) Systematics of the Guiana shield margin segments as determined by the present study including the rift obliquity angles and segment labels. FOZ, Foz d'Amazonas; FZ, transform fracture zone; GS, Guiana-Suriname; TM, transform margin.

## 2.2. Central Atlantic Rift-Guiana-Suriname Basin

The CAR initiated in the Morocco/New Scotland region in the Triassic and propagated southward to the present-day location of the Demerara Plateau (Klitgord & Schouten, 1986; Labails et al., 2010; Schettino & Turco, 2009). Some authors suggested that the Takutu rift, located within the Guiana Shield (Figure 1b), corresponds to the southernmost abandoned tip of the CAR, although its kinematic relationships to the CAR remain unclear (Crawford et al., 1985; McConnell, 1969; Szatmari, 1983).

The exact timing of the CAR is not very well constrained in the studied area. It occurred from the Late Triassic to the Early Jurassic in the Takutu rift and Guinea Plateau (Figure 1a; Crawford et al., 1985; Marinho et al., 1988; McConnell, 1969). Several kinematic reconstructions dated the rifting to the Early Jurassic (Benkhelil et al., 1995; Pindell & Kennan, 2009; Schettino & Turco, 2009). Basile et al. (2020) reported syn-rift magmatism ca. 173 Ma in the Demerara Plateau. Pindell (1985) suggested the accretion of oceanic crust in the Middle Jurassic (Bathonian, 170–172 Ma) overlaid by Callovian-Oxfordian sediments (166–157 Ma; Nemčok et al., 2016). The Central Atlantic break-up unconformity (CABU) was tentatively ascribed by Crawford et al. (1985) a Mid-Jurassic age (ca. 176–172 Ma) assuming the Takutu rift is related to the CAR (Figure 1b).

Besides, syn-rift deposits of the GS basin have a reflectivity pattern that would be suggestive of seaward dipping reflectors (SDR) of magmatic origin (e.g., Museur et al., 2020; Nemčok et al., 2016; Reuber et al., 2016). The Jurassic oceanic crust of the GS basin is thicker than average (>12 km), suggesting higher than normal melt accretion to produce that oceanic crust (e.g., Reuber et al., 2016) potentially related to the Sierra-Leone hotspot (Basile et al., 2020). In any case, these considerations show that Jurassic rifting was therefore associated with mantle magmatism.

## 2.3. Equatorial Atlantic Rifting -Demerara Plateau and Foz d'Amazonas Basin

The Equatorial Atlantic Ocean is bounded by the Doldrums and the Chain FZ (e.g., Basile et al., 2005; Mercier de Lépinay, 2016; Ye et al., 2017; Figure 1). The EAR initiated in the Barremian (i.e., the age of syn-rift

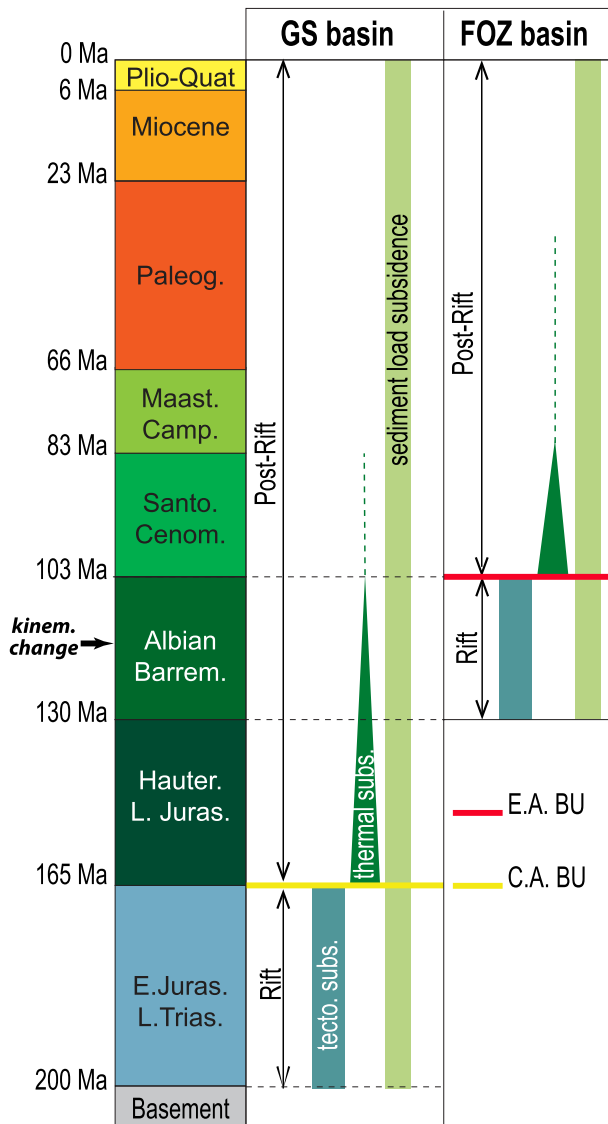


**Figure 3.** Stratigraphic chart showing the horizons interpreted on the seismic data, the main geodynamic stages for the Guiana-Suriname (GS) and Foz do Amazonas (FOZ) basins and the main mechanisms assumed to drive the subsidence. BU, break-up unconformity; CA, Central Atlantic; EA, Equatorial Atlantic.

sediments in the FOZ and Marajo basins; Brandão & Feijó, 1994; Figueiredo et al., 2007; Zalán & Matsuda, 2007). Oblique rifting formed an en-échelon system of dextral pull-apart basins (e.g., Benkhelil et al., 1995; Guiraud et al., 1992; Mascle et al., 1988; Ye et al., 2017). The Equatorial break-up unconformity (EABU) and first oceanic crust are considered as Albian in age (ca. 107–100 Ma) east of the Demerara Plateau (Sapin et al., 2016; Loncke et al., 2020; Mercier de Lépinay, 2016), in the FOZ basin (Brandão & Feijó, 1994; Figueiredo et al., 2007), in the Marajo basin (Zalán & Matsuda, 2007) and along the conjugate African margin (Mascle & Blarez, 1987; Moullade et al., 1993; Ye et al., 2017). Some authors consider the oceanic crust is slightly younger (Aptian; Basile, 2015). Whatever the exact age of rifting, continental break-up in the pull-apart basins formed isolated “oceanic crust basins” separated by transforms (Basile et al., 2005; Gillard et al., 2017; Ye et al., 2017) that ultimately coalesced (Figure 1a).

Equatorial Atlantic rifting overlapped in time with a Late Aptian-Albian reorganization in plate kinematics induced by a change of rotation pole of Africa with respect to South-America. This event induced a transition in the extension direction between Africa and South America from ESE to E-W between 112 and 105 Ma (Basile et al., 2013; Benkhelil et al., 1995; Campan, 1995; Rabinowitz & LaBrecque, 1979).

By contrast with the CAR, little magmatism has been documented during the development of the EAR, which is only reported along the eastern border of the Demerara plateau (120–125 Ma; Greenroyd et al., 2008; Loncke et al., 2009) as well along the conjugated Guinea Plateau (late Albian: ca. 100 Ma; Olyphant et al., 2017). Mid-Cretaceous oceanic crust under the FOZ basin is thinner than average (3.5–5 km; Greenroyd et al., 2007; Rodger et al., 2006; Watts et al., 2009). This has been related either to a slow spreading rate of the oceanic ridges (Rodger et al., 2006; Watts et al., 2009)—although some authors consider the ridge to be rapid (Rabinowitz & LaBrecque, 1979; Nemčok et al., 2016)—or to the fact that fracture zones and associated tip ridges are closely spaced in the FOZ basin (Greenroyd et al., 2007).

### 3. Method

#### 3.1. Data Set

We interpreted a grid of 2D seismic reflection located between the Caribbean subduction front and the Saint Paul FZ (Figures 2 and S1). We calibrated our seismic interpretations using 33 wells located in the shelf and bathyal domains (Figure S1). We used this seismic grid to map the

continental crust structure as well as 9 stratigraphic horizons across the studied area (Figure 3). Crustal thickness was estimated from two-way-travel-time to depth conversion using velocity ranging from 5.5 to 7.5 m/s for the continental crust and 5.5–7.7 km/s for the oceanic crust.

#### 3.2. Mapping of Crustal Domains

We mapped five types of crustal domains using definitions of Peron-Pinvidic et al. (2013), Sutra et al. (2013) and Ye et al. (2019). Among criteria detailed in Table 1, the proximal domain was mapped where minor extension is accommodated by normal/strike-slip faults and/or the (pre-rift) continental crust (CC) is only weakly thinned (crustal thickness >25 km) with respect to the onshore cratonic domain (~42 km; Table 1). The necking domain (ND) was mapped where the (pre-rift) continental crust is significantly thinned (i.e.,

**Table 1**

*Definitions of Crustal Domains Mapped From the Seismic Data-Base (Modified After Peron-Pinvidic et al., 2013, Sutra et al., 2013, and Ye et al., 2019)*

Proximal domain (PD)	<ul style="list-style-type: none"> <li>• Minor extensional features (high angle and listric faults)</li> <li>• Often wedge-shaped sedimentary strata</li> <li>• Weak thinning of the pre-rift CC (thickness &gt;25 km)</li> </ul>			
Necking domain (ND)	<ul style="list-style-type: none"> <li>• Drastic thinning of the pre-rift CC (from 25 to 10 km)</li> <li>• Detachment faults</li> <li>• Significant upwelling of the Moho</li> <li>• Maximum thickness of syn-rift wedges</li> <li>• Sealed by the BU</li> <li>• Often the long-term location of the shelf edge of the late post-rift wedge</li> </ul>			
Hyper extended domain (HED): Magma poor segment	<table border="0"> <tr> <td style="vertical-align: top;"> <ul style="list-style-type: none"> <li>• Very thin CC (&lt;10 km)</li> <li>• Offset of the Moho by syn-rift faults</li> <li>• Sealed by the BU</li> <li>• Sag type sedimentary depocenters</li> <li>• Low reflectance within the crust</li> </ul> </td> <td style="vertical-align: top; text-align: center;">           Distal margin domain (DM): Magma rich segment         </td> <td style="vertical-align: top;"> <ul style="list-style-type: none"> <li>• Very thin CC (&lt;10 km)</li> <li>• Offset of the Moho by syn-rift faults</li> <li>• Sealed by the BU</li> <li>• Low reflectance within the CC</li> <li>• High reflectance reflectors in the syn-rift deposits and SDR</li> <li>• Widely distributed curved and merging features in the lower CC</li> <li>• Often underplating features</li> </ul> </td> </tr> </table>	<ul style="list-style-type: none"> <li>• Very thin CC (&lt;10 km)</li> <li>• Offset of the Moho by syn-rift faults</li> <li>• Sealed by the BU</li> <li>• Sag type sedimentary depocenters</li> <li>• Low reflectance within the crust</li> </ul>	Distal margin domain (DM): Magma rich segment	<ul style="list-style-type: none"> <li>• Very thin CC (&lt;10 km)</li> <li>• Offset of the Moho by syn-rift faults</li> <li>• Sealed by the BU</li> <li>• Low reflectance within the CC</li> <li>• High reflectance reflectors in the syn-rift deposits and SDR</li> <li>• Widely distributed curved and merging features in the lower CC</li> <li>• Often underplating features</li> </ul>
<ul style="list-style-type: none"> <li>• Very thin CC (&lt;10 km)</li> <li>• Offset of the Moho by syn-rift faults</li> <li>• Sealed by the BU</li> <li>• Sag type sedimentary depocenters</li> <li>• Low reflectance within the crust</li> </ul>	Distal margin domain (DM): Magma rich segment	<ul style="list-style-type: none"> <li>• Very thin CC (&lt;10 km)</li> <li>• Offset of the Moho by syn-rift faults</li> <li>• Sealed by the BU</li> <li>• Low reflectance within the CC</li> <li>• High reflectance reflectors in the syn-rift deposits and SDR</li> <li>• Widely distributed curved and merging features in the lower CC</li> <li>• Often underplating features</li> </ul>		
Intruded continental crust (ICC)	<ul style="list-style-type: none"> <li>• Between CC and OC</li> <li>• CC shows strong internal reflectance that might correspond to magmatic intrusions</li> <li>• Unclear Moho reflection</li> <li>• Sealed by the BU</li> </ul>			
Oceanic domain (OC)	<ul style="list-style-type: none"> <li>• Strong reflection of the Moho</li> <li>• Often a local downwelling of the Moho (thickening of the proximal OC)</li> </ul>			

Abbreviations: BU, break-up unconformity; CC, continental crust; HED, hyperextended domain; ICC, intruded continental crust; ND, necking domain; OC, oceanic domain; SDR, seaward dipping reflector.

down to ~10 km in thickness; Table 1). The distal part of the margin, where the (pre-rift) continental crust is extremely thinned ( $\leq 10$  km), has been mapped as one of two types. Without indication of significant magmatism during rifting, it has been mapped as hyper-extended domain (HED; Table 1). Alternatively, where crustal thinning was potentially associated with magmatism (i.e., includes SDR), it has been mapped as the distal margin domain (DM, Table 1). The transition between continental and oceanic crust, where the crust shows strong internal reflectance that might correspond to magmatic intrusions and/or the reflection of the base of the crust (Moho) is not clear, has been mapped as an intruded continental crust (ICC; Table 1). Finally, the oceanic domain was mapped where the top of the basement and the Moho show a strong reflectance (OC; Table 1).

The subsurface data-set density permitted mapping the crustal structure in details throughout the study area. In the following, we illustrate the crustal structure with 8 cross-sections although the results illustrated below have been established using the complete data set.

### 3.3. Obliquity of Margin Segments

We classified margin segments according to their obliquity to the rift extension direction. Following Ye et al. (2019), the margin segment obliquity was determined from the angle between the directions of the transform faults and of the direction of the segment (Figure 2). The margin segment direction was estimated by the direction of the continent-ocean boundary as mapped from seismic data. The rift extension direction was estimated from the direction of the transform structures. In the GS basin, the obliquity has

been measured with respect to the Jurassic Guiana transform margin (Guiana TM; Pindell, 1985; Pindell & Kennan, 2009; Figure 2). In the FOZ basin, the obliquity has been measured with respect to the transform directions taken only near the continent-oceanic crust transition mapped by Cordani et al. (2016). Indeed, these directions actually track the original rift extension direction, that is, before the mid-Cretaceous plate kinematic change. We used the classification of Mercier de Lépinay et al. (2016) and Ye et al. (2019) for whom obliquity of transform margin segments ranges from  $0^\circ$  to  $15^\circ$ , oblique margin segments from  $15^\circ$  to  $75^\circ$  and divergent margin segments  $>75^\circ$  (Figure 2).

## 4. Results

### 4.1. General Structure of the Guiana Passive Margin

Our mapping shows that the GS basin developed upon an NNE-trending divergent margin segment (i.e., D1 segment forming the western boundary of the Demerara Plateau) and ESE-trending transform to highly oblique margin segments in the South (i.e., T1 and O1 segments along Guiana TM; Figure 2). Conjugates of those margin segments are now found in the Gulf of Mexico and southern Florida/Bahamas, respectively (Pindell, 1985; Pindell & Kennan, 2009).

In the domain where thinning resulted from Equatorial Atlantic Rifting, the northern boundary of the Demerara Plateau is formed by ESE-trending transform segments (i.e., T2 and T3 along the Sierra-Leone fracture zone). The eastern boundary of the Demerara Plateau is a N-trending divergent segment (i.e., D2; Figure 2). Further East, the western part of the FOZ basin formed upon an ESE-trending transform segment (i.e., T4 segment along the Four North fracture zone) and two SE-trending oblique segments (i.e., O2, and O3 segments) bounding a N-trending divergent one (i.e., O3 segment; Figure 2). Conjugates of those segments are the Guinea—Liberia segments of the African margin (e.g., Benkhelil et al., 1995; Loncke et al., 2009; Ye et al., 2019; Figure 1a).

Thus, our mapping shows that the margin of the Guiana Shield has a complex geometry with segments typically a few hundreds of km in length, with contrasting directions (from NS to ESE trending) and alternating obliquities between transform, oblique and divergent segments. This pattern is consistent in the EAR domain with the mapping established by Ye et al. (2017, 2019) for the conjugated African margin.

### 4.2. Western Demerara Plateau and Guiana-Suriname Basin

#### 4.2.1. D1 Divergent Segment

The eastern part of the GS basin overlies the transition from the Demerara plateau continental crust to the Central Atlantic Jurassic oceanic crust (segment D1; Figures 2 and 4a). Crustal thinning is accommodated, from East to West, by (a) a wide crustal necking domain (ca. 190 km wide) without well imaged normal faults but with features suggesting extensional deformation in the lower crust marked essentially by low-angle anastomosed lens-shaped shear patterns (see Clerc et al., 2015, 2018; Figure 4a), (b) a distal margin domain ( $>100$  km wide) with tilted crustal blocks bounded by continent-ward dipping normal faults (CDNF; Clerc et al., 2018) rooted in a thick sheared lower crust, and, (c) a narrower continent-ocean transition domain (intruded continental crust;  $<70$  km wide; Figure 4a). The syn-rift deposits form a crustal-scale west dipping wedge. They are thickest in the necking and distal margin domains, that is, where tectonic subsidence created the maximum of accommodation (Figure 4a; Table 1). As mentioned above, these deposits, showing seaward dipping reflector (SDR), might be of magmatic origin (Basile et al., 2020; Museur et al., 2020; Nemčok et al., 2016; Reuber et al., 2016) and subaerial (Basile et al., 2020; Planke et al., 2000). Thus, whether detrital, magmato-volcanic or both, these syn-rift deposits probably correspond to continental/shallow environments, suggesting that accommodation was continuously filled up to compensate for tectonic subsidence.

Break-up and oceanic accretion took place west of the main syn-rift depocenter (necking domain and distal margin; Figure 4a). The top of the Jurassic syn-rift is truncated by an unconformity, most probably the CABU (Figures 3 and 4a). Above that unconformity, a carbonate platform developed along the western boundary of the syn-rift basin (e.g., Staatsolie, 2013; Figure 4a). This indicates a low clastic input to the margin at the time. Above, renewed clastic inputs formed the Barremian-Albian sedimentary wedge

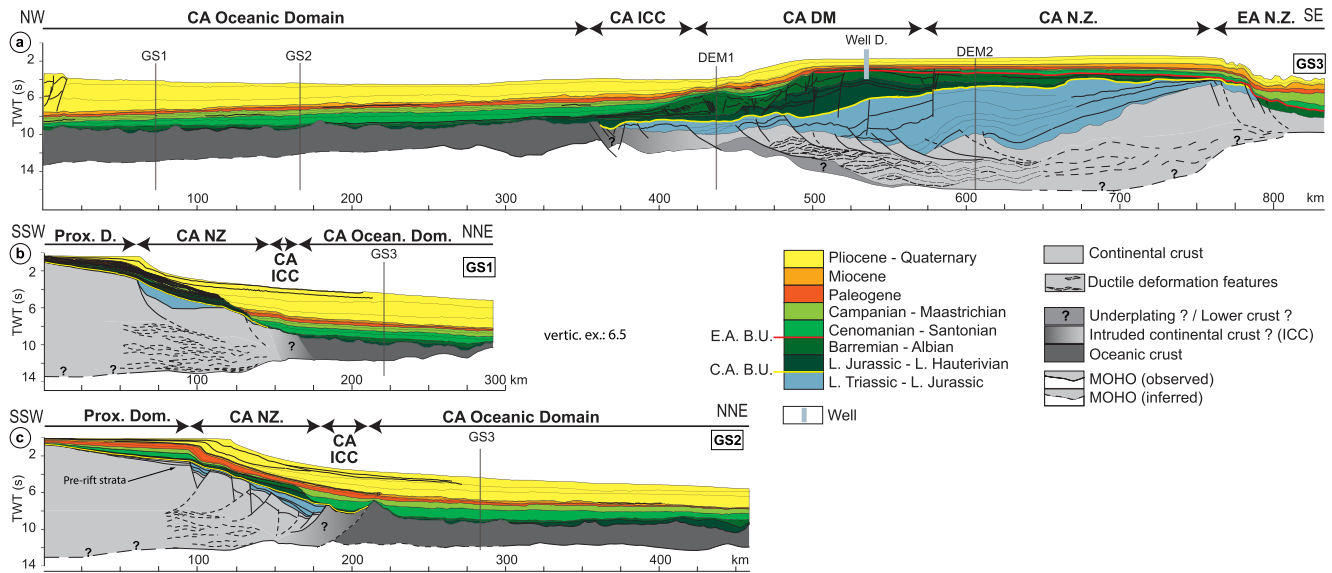


**Figure 4.** Geological cross sections across the (a) D1, (b) T1, and (c) O1 segments of Guiana-Suriname basin. See location on Figure 2. CA, Central Atlantic; DM, distal margin; EA, Equatorial Atlantic; ICC, intruded continental crust; ND, necking domain.

(130–100 Ma), which underwent a major westward gravitational collapse event that formed an upslope extensional domain and a downslope compressional domain (Figure 4a).

Subsequent post-rift clastic systems are mostly indicative of a long-term aggrading trend although their depocenters progressively migrated westward, into the distal margin domain and onto the oceanic crust. Thin Paleogene and Miocene deposits indicate a reduced clastic input to the GS basin between ca. 66 and 6 Ma that was then renewed in the Pliocene, which is significantly thicker. Pliocene deposits thicken westward as they are progressively involved in the accretionary prism (Figure 4a).

#### 4.2.2. T1 Transform Segment and O1 Oblique Segment

Across the southwestern boundary of the GS basin, crustal thinning is accommodated through a narrow necking domain (ca. 80–90 km wide) with normal faults in the upper crust and a ductilely deformed lower crust (Figures 4b and 4c). As a difference with the D1 segment, the volume of syn-rift deposits is here limited, with no SDR imaged. As along the D1 segment, the syn-rift infillings are overlain by Upper Jurassic platform carbonates and Lower Cretaceous clastics. Post-rift deposits are preserved across the entire margin but truncations in the necking domain disconnect the proximal and distal parts of the sedimentary wedges (Figures 4b and 4c). The Pliocene wedge is thick (>4 s) and is not truncated in the necking domain.

### 4.3. Northern and Eastern Demerara Plateau and Western Foz do Amazonas Basin

#### 4.3.1. T2 and T3 Transform Segments

North of the Demerara Plateau, the EAR necking domain is imaged at the northernmost end of sections DEM1 and DEM2 (Figures 2 and 5). The remaining southern portions of those lines actually image an along-strike section of the Central Atlantic necking domain and its Jurassic syn-rift wedge described above (Figures 2 and 5).

Along segments T2 and T3, the necking domain is only 20–25 km wide and accommodated by ocean-ward dipping normal faults (ODNF; Clerc et al., 2018) that are not well imaged at depth (Figure 5). The volume of syn-rift deposits is limited (Figure 5). The Early Cretaceous post-rift deposits show evidence of fault reactivation corresponding to transpressional deformation documented along the Demerara—Guinea plateaus boundary related to the kinematic change from WNW-ESE to E-W rifting direction between 112 and 105 Ma (Figure 5; Basile et al., 2013). Above, post-rift clastic sedimentary wedges are truncated in the necking domain, separating a proximal and a distal depocenter, as documented along the T1 transform segment

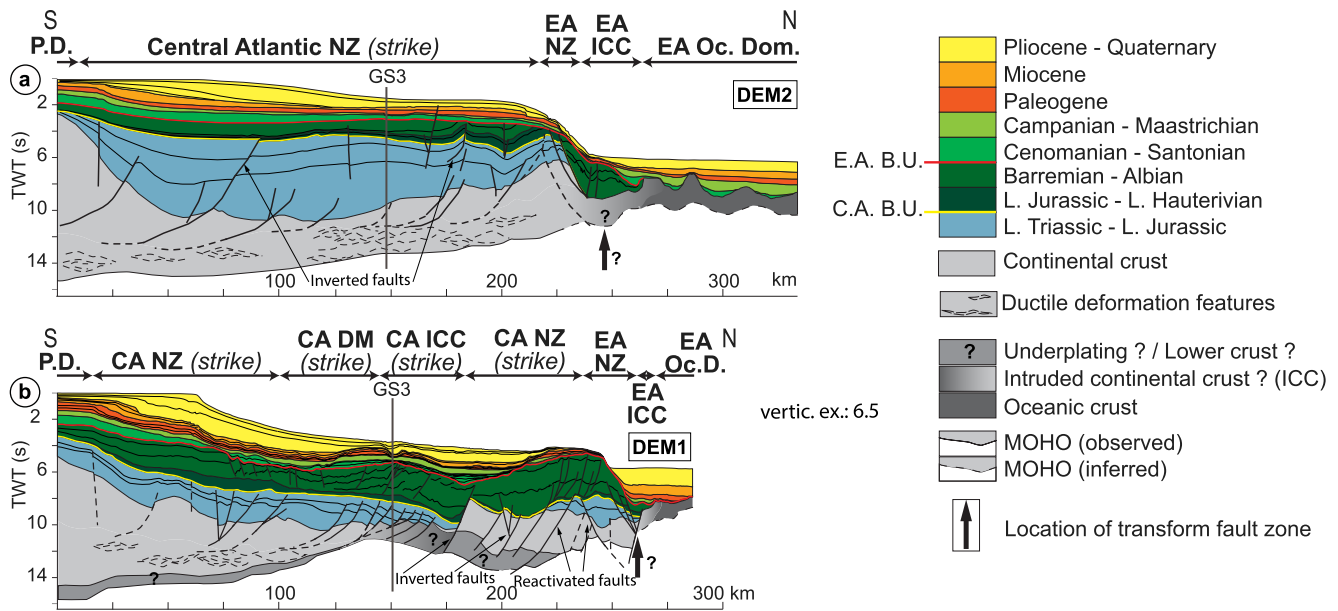


**Figure 5.** Geological cross sections through the northern edge of the Demerara Plateau across the (a) T2 and (b) T3 transform segments. See location on Figure 2. CA, Central Atlantic; EA, Equatorial Atlantic; HED, hyper extended domain; ICC, intruded continental crust; ND, necking domain.

(Figures 4b and 5). Paleogene and Miocene (66–6 Ma) deposits have a reduced thickness (<1 s). In the Pliocene, a prograding wedge on top of the Demerara plateau that could have been fed by the Maroni River while the distal part of the margin received supply from the Amazon River (Figure 5).

#### 4.3.2. D2 Divergent Segment

Segment D2 is imaged in the easternmost part of the GS3 section (Figure 4a). The EAR necking domain is ca. 75 km wide and accommodated by ODNF (e.g., Sapin et al., 2016; Figure 4a). The volume of syn-rift sediment is reduced, except for a local depocenter at the juncture of the divergent and the transform segments shown by Sapin et al. (2016). Above, only the first post-rift clastic sediment wedges are truncated in the necking domain, although subsequent Cretaceous and Cenozoic deposits show many canyon incisions and mass transport complexes (MTC) in the proximal domain (Figure 4a). Above an unconformity sealing Cretaceous deposits, a wide carbonate platform developed during the Paleogene and Miocene (e.g., Hoorn et al., 2010; Sapin et al., 2016; Yang & Escalona, 2011). This indicates a low clastic input to the margin between ca. 66 and 6 Ma (van Soelen et al., 2017). The Pliocene wedge thickens oceanward as it is in part fed by the modern Amazon River (e.g., Basile et al., 2013; Sapin et al., 2016; Figure 4a).

#### 4.3.3. O2 Oblique Segment and D3 Divergent Segment

In the western FOZ basin, the O2 segment is illustrated with a dip section (Figures 2b and 6a). Bedding patterns in the pre-rift of the proximal domain suggest some extensional deformation prior to the Equatorial Atlantic rifting (Figures 6a and 6b). Similar beddings pre-dating the EAR have been documented in the southeastern Demerara Plateau (e.g., Basile et al., 2005; Brandão & Feijó, 1994; Figueiredo et al., 2007), in the Marajo basin (e.g., Costa et al., 2002), the FOZ basin (e.g., Milani et al., 2007), as well as along the conjugate Guinea-Liberia segment and further East along the African margin (Sierra Leone-Liberia, Ivory Coast, Ghana and Benue basins; see Bennett & Rusk, 2002; Guiraud, 1993; Marinho et al., 1988; Mascle et al., 1988; Olyphant et al., 2017; Ye et al., 2017, 2019). This suggests that this EAR segment developed along an aborted branch of the CAR (Benkhelil et al., 1995; Ye et al., 2017).

Along the O2 oblique segment, the necking domain is ca. 40–50 km wide, without clearly imaged normal faults and with only a few features indicative of ductile deformation in the lower crust (Figure 6a). The hyper-extended domain is 65 km wide and accommodated by CDFN (Figure 6a). Along the D3 divergent segment, the necking and hyper-extended domains are wider (ca. 100 and 110 km respectively) and thinning is accommodated by ODNF (Figure 6b). In the western FOZ basin, the syn-rift deposits are clastics

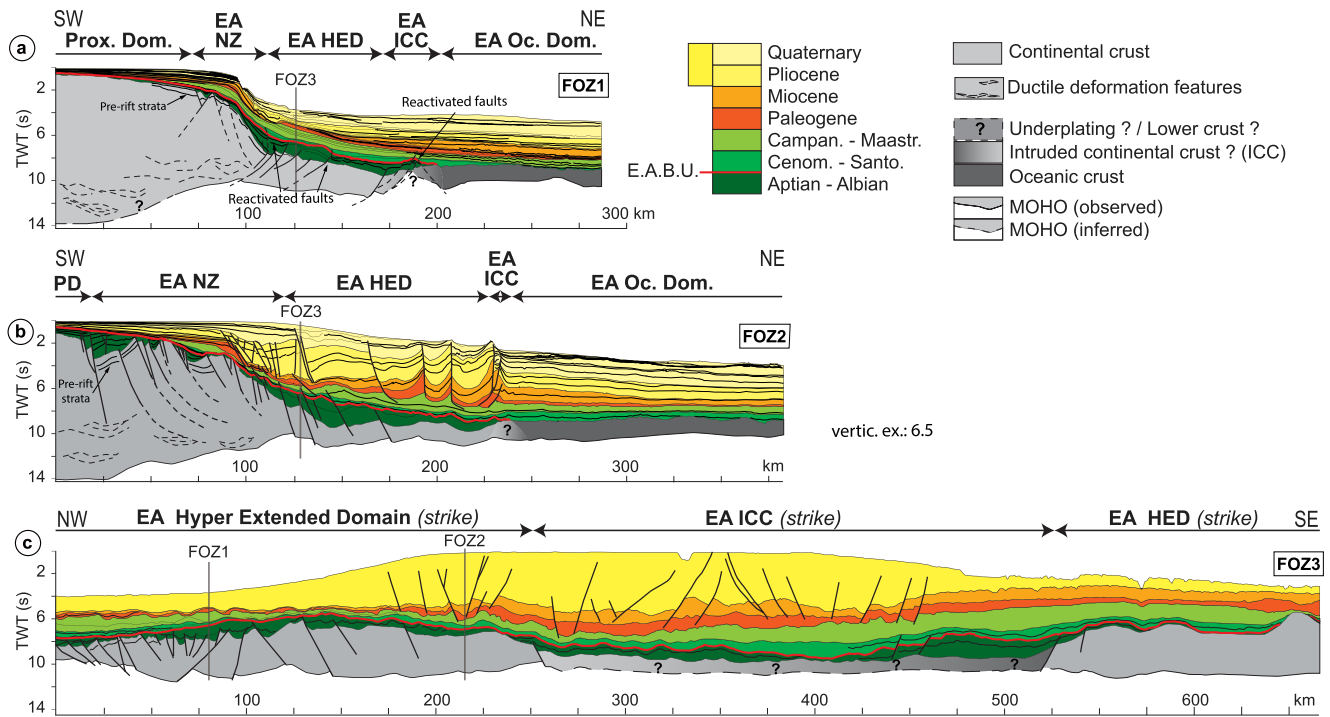


**Figure 6.** Geological cross sections through the (a) O2 and (b) D3 segments of the FOZ basin. (c) Strike section along the O3 segment across the Amazon delta. See location on Figure 2. CA, Central Atlantic; EA, Equatorial Atlantic; HED, hyper extended domain; ICC, intruded continental crust; ND, necking domain.

deposited mostly in continental or shallow marine environment (Sapin et al., 2016). They are truncated by the EABU above which post-rift deposits are widely spread from the proximal domain to the oceanic domains. Cenomano-Santonian deposits (ca. 103–83 Ma) show evidence of fault reactivations (Figure 6a). Reactivation, probably driven by a change in plate vectors, is coeval with transpressional deformation along the Romanche FZ during the Santonian (Davison et al., 2016; Destro et al., 1994; Zalán et al., 1985) as also documented along the African margin (Antobreh et al., 2009; Attoh et al., 2004; Ye et al., 2017). Upper Cretaceous sediments (83–66 Ma) were deposited evenly across the margin after planation of its reliefs. From the Early Paleocene (ca. 66 Ma) onward, deposits become thicker in the oceanic domain and show truncations in the necking domain (Figures 6a and 6b). Clastic input reduced during the Paleogene and the margin became starved during the Neogene, allowing for the development of a carbonate platform (Figueiredo et al., 2007; Hoorn et al., 1995). The clastic input is renewed in the Pliocene with the Amazon Delta burying the carbonate platform under very thick series (~2.5–3 s; i.e., 3–3.5 km; Figures 6b and 6c). The delta formed after the establishment of the modern course of the Amazon River in the Late Miocene, routing sediments from the Andean foreland through the Amazonian plains to the FOZ basin (e.g., Hoorn et al., 1995; Shephard et al., 2010; van Soelen et al., 2017). The delta displays spectacular gravity driven deformation features (upslope extensional domain and downslope fold-and-thrust belt) rooted in a Paleogene décollement layer (Figures 6b and 6c).

## 5. Discussion

### 5.1. Kinematic Context of Crustal Thinning

Our observations of the crustal and stratigraphic structure along the Guiana Shield margin illustrate the segmentation of the margin in terms of orientation, width and obliquity of the segments. In order decipher the respective contributions of the successive rifting events (CAR and EAR), their local superimposition, and their contrasting kinematics (southern tip of the CAR vs. highly oblique EAR) to the segmentation pattern, we integrated our results into a consistent and evolving large-scale kinematic framework. In order to compile these maps, we combined our results with the plate kinematic canvases of Moulin et al. (2010)

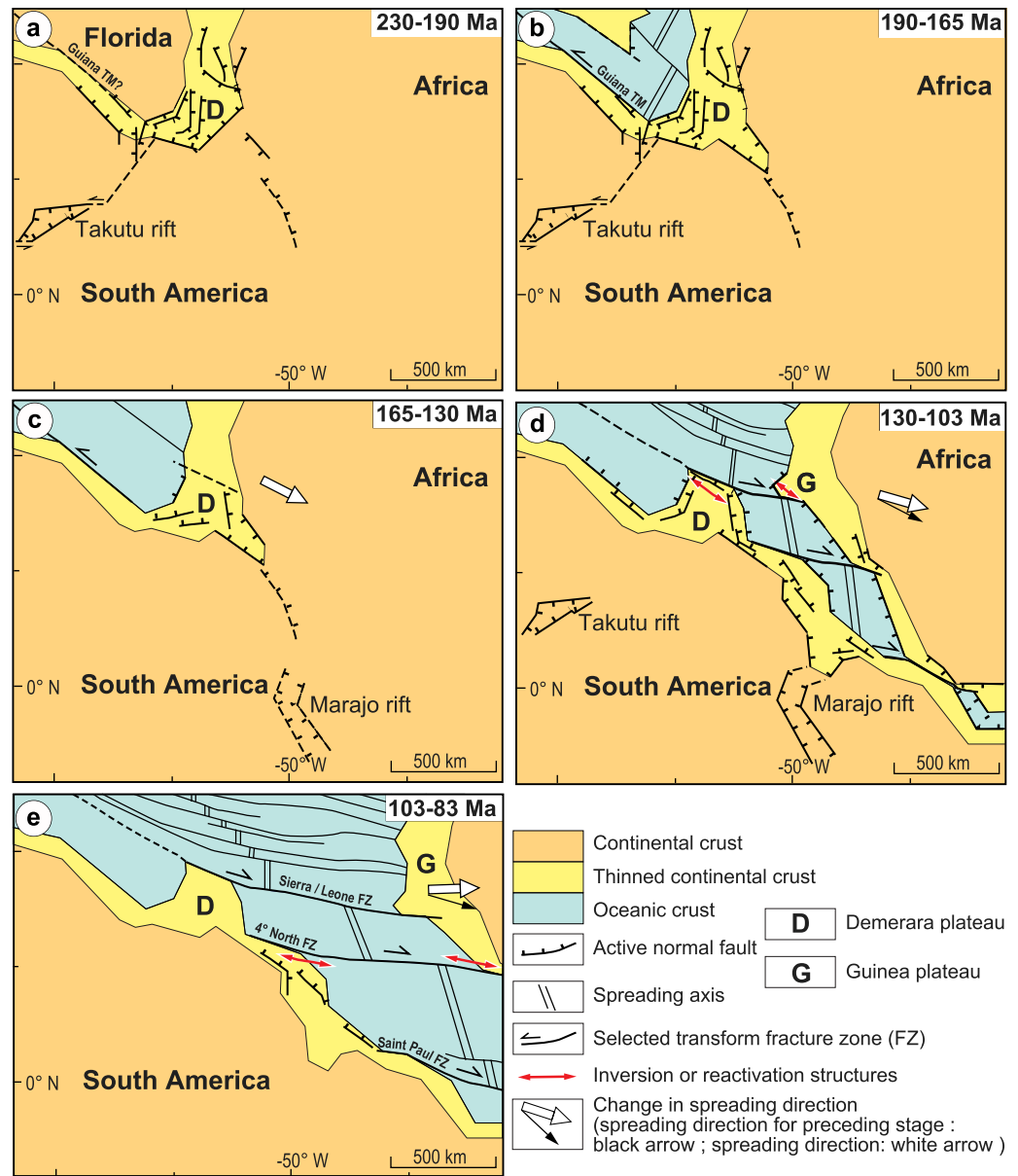


**Figure 7.** Schematic evolution in map view of crustal thinning along the Guiana Shield margin as determined in this work. Crustal deformation along the conjugated African Margin after Ye et al. (2017, 2019; and references therein). Kinematic framework after Benkhelil et al. (1995), Moulin et al. (2010), Pindell and Kendall (2009) and Ye et al. (2017). (a) 230–190 Ma: Central Atlantic rift. (b) 190–165 Ma: Central Atlantic break-up and accretion. (c) 130–103 Ma: Central Atlantic post-rift. (d) 130–103 Ma: Equatorial Atlantic rift, break-up and accretion. (e) 103–83 Ma: Equatorial Atlantic post-rift. FZ, transform fracture zone; TM, transform margin.

and Pindell and Kennan (2009). For the crustal thinning pattern along the conjugated African margin, we used the work of Ye et al. (2017, 2019).

During the Triassic and Early Jurassic (ca. 230–190 Ma), we showed that thinning initiated in a wide (>300 km) NNE-trending rift system at the location of the present-day Demerara Plateau, that is, at the southern tip of the CAR and a narrow NW-SE branch along the Guiana TM (<90 km; Figures 4a and 7a). Our mapping suggests that this rift was associated with a SE-trending branch that did not reach break-up between the future FOZ segments of the Guiana shield margin and their Guinea-Liberia conjugates (Figure 7a).

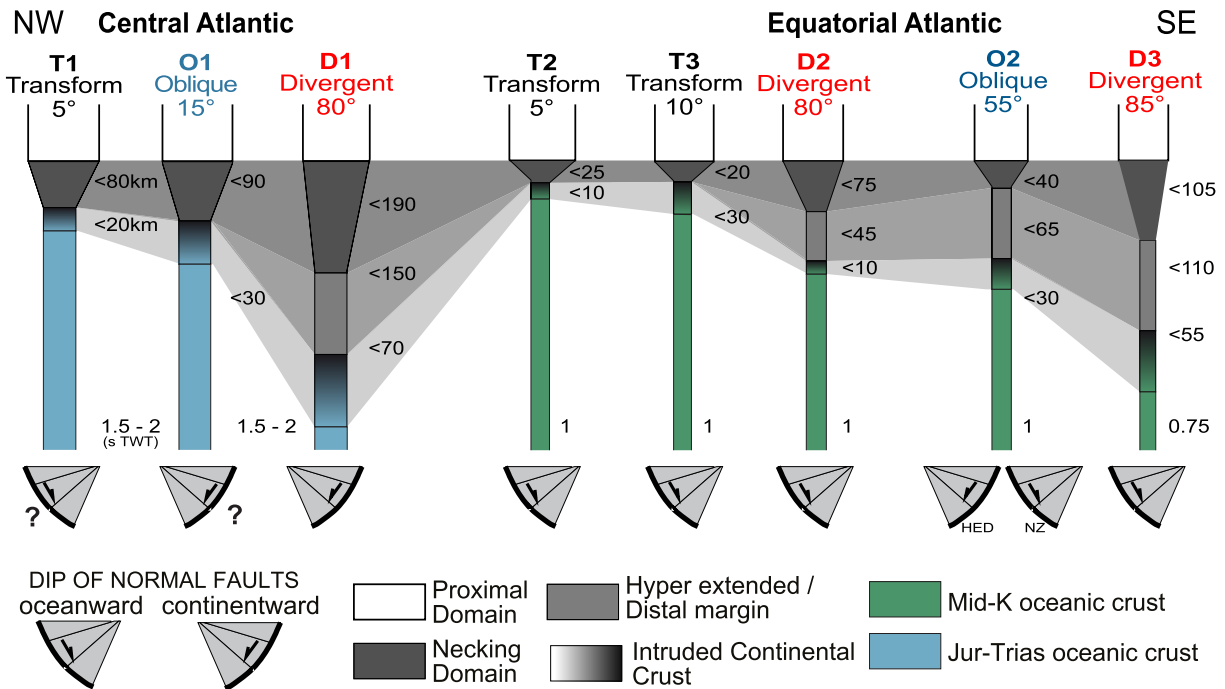


**Figure 8.** Summary of the main crustal structure characteristics of the Guiana shield margin segments. Values are dip width of the crustal domains in km except for the oceanic crust for which the thickness in TWT in seconds is indicated. See location of segments on Figure 2.

During the Late Jurassic and Early Cretaceous (ca. 190–130 Ma), our mapping indicates that the CAR lithospheric break-up and oceanic accretion took place to the NW of the Demerara Plateau and formed a wide divergent (D1) and narrow transform (T1)/oblique (O1) margin segments of the GS basin (Figures 2, 4 and 7b). This thinning also propagated further to the SE in a NW-trending trough, as well as in the Marajo basin (Figures 7b and 7c).

Later in the Early Cretaceous (ca. 130–103 Ma), the EAR developed as an en-échelon rift system and our observations suggest that it propagated along the aborted branches of the CAR between the Demerara Plateau and in the Marajo basin (Figures 6 and 7). The EAR extension evolved into break-up with oceanic accretion in isolated basins partly accommodated by transforms and ultimately formed the highly segmented margin (Figure 7d). During that period, the kinematic change in South America-Africa relative plate motion produced transpressional features at the edges of the Demerara and Guinean Plateaus (Figures 3 and 7d).

In the Late Cretaceous (ca. 103–83 Ma), transforms accommodated further accretion and initially isolated oceanic crust domains coalesced (Figure 7e). Ongoing counterclockwise rotation of the African plate produced transpressional features along the 4° North transform (Figure 7e).

## 5.2. Spatial Distribution of Necking Style

Our observations also illustrate the variability of the necking style of the margin segments (necking domain width and occurrence of a hyper-extended or distal margin domain) along the Guiana Shield margin. Here we synthesize these observations for each segment (Figure 8) and provide a map of the crustal domains and the main deformation structures at the scale of the studied area (Figure 9).

### 5.2.1. Necking Width and Obliquity

In the CAR domain (where thinning results from the Jurassic rifting), the necking domain is very narrow (80–90 km) along the T1 transform and O1 oblique segments (Figures 8 and 9). It becomes laterally much wider (190 km) along the D1 divergent segment where it is associated with a distal margin domain, further amplifying the difference in the margin width between the divergent and transform segments (Figures 8 and 9).

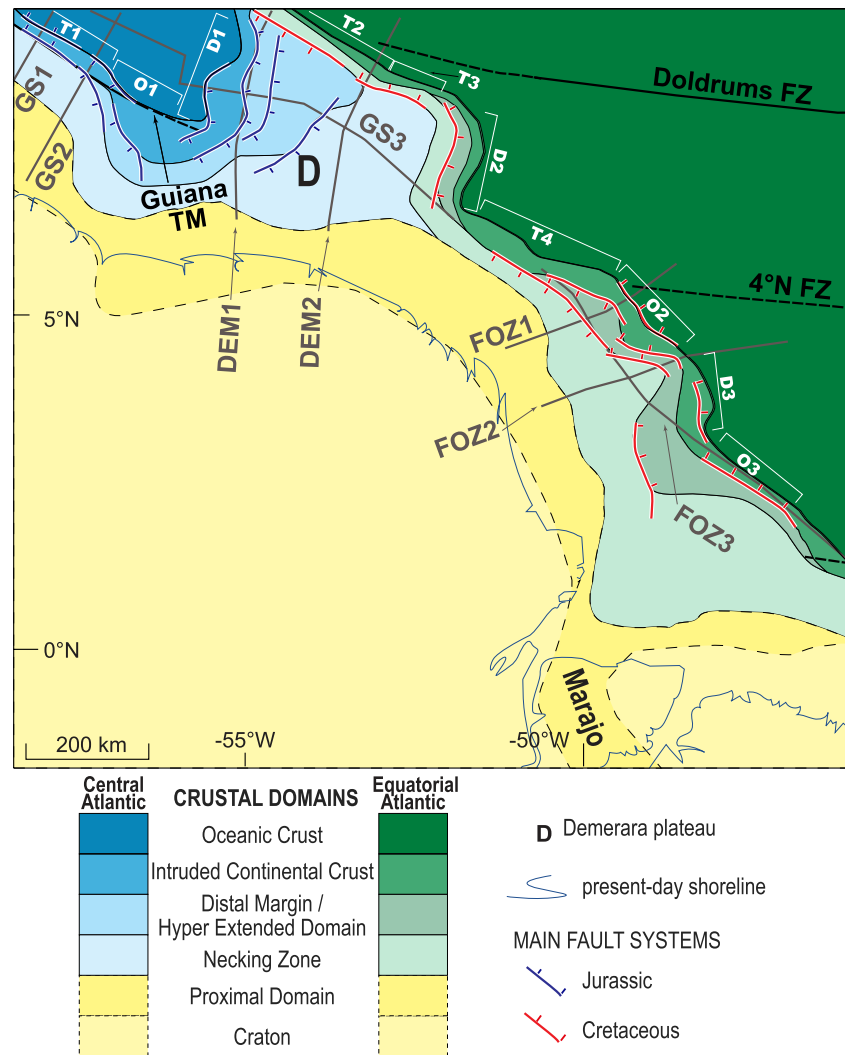


**Figure 9.** Crustal domains map of the study area constructed from the full data set (Figures S1 and S2). Central Atlantic rifting crustal domains are shown in blue and Equatorial Atlantic rifting crustal domains in green. Location of cross-sections of Figures 4–6 are shown in dark gray. Margin segment labels are shown in white. FZ, transform fracture zone; TM, transform margin.

In the Equatorial Atlantic domain (where thinning results from the Cretaceous rifting), the necking domain is very narrow (20 km) without hyper-extended domain along the T2/T3 transform segments of the Demerara Plateau (Figures 8 and 9). The necking domain becomes laterally wider (75 km) with an associated hyper-extended domain along the D2 divergent segment (Figures 8 and 9). The hyper-extended domain disappears along the T4 transform segment and reappears along the O2 oblique segment (Figures 8 and 9). The width of the necking and hyper-extended domains widens progressively along the O2 oblique and D3 divergent segments (ca. 105 and 115 km; Figures 8 and 9).

Our observations show that divergent segments are consistently wider than oblique or transform segments (Figures 8–10). This relationship is also true along the conjugate African margin (Ye et al., 2019; Figure 10) and actually, worldwide (e.g., Jeannot & Buiter, 2018). Moreover, both numerical and analog modeling have shown that the higher the rift obliquity the narrower the rift (e.g., Brune et al., 2012; Tron & Brun, 1991). The rift width undoubtedly controls the necking domain of resulting rifted margins after break-up.

After break-up, our mapping shows that the width of the crustal thinning then controls the slope of the sedimentary systems throughout the evolution of the rifted margin. Indeed, narrow transform segments show

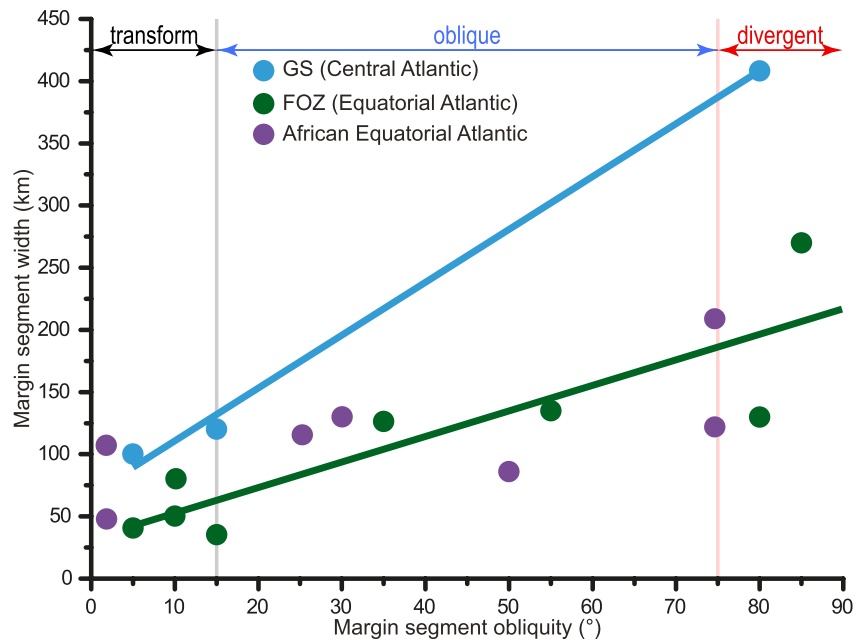


**Figure 10.** Relationship between the margin width (necking domain plus hyper-extended domain/distal margin) and obliquity of the studied margin segments as determined in this study. Central Atlantic segments are shown in blue (GS, Guiana-Suriname). Equatorial Atlantic segments are shown in green (FOZ, Foz do Amazonas). African Equatorial Atlantic are shown in purple (after Ye et al., 2019).

steep continental slopes throughout their post-rift history and the sedimentary wedges are systematically truncated in the necking domain by gravity driven sedimentary processes (erosion and mass transport).

### 5.2.2. Necking Width and Atlantic Rift Domains

The Equatorial Atlantic margin segments are systematically narrower than Central Atlantic margin segments (Figure 10). This can be attributed to several, non-mutually exclusive causes. As previously pointed out, the width of the crustal thinning domain depends on the obliquity of the rift extension direction. Global kinematic reconstructions show that the extension direction of the EAR was indeed significantly more oblique (10°–30°) than that of the southern tip of the CAR (80°–70°; Brune et al., 2018). Also, the width of a rift depends on the extension rates as well, with wider rift and rifted margins, for slower rates (e.g., Brune et al., 2018; Svartman Dias et al., 2015). Global kinematic reconstructions show that the full-rift velocities of the EAR were indeed faster (up to 30 m/My) than for the southern tip of the CAR (16–20 m/My; Brune et al., 2016). Finally, numerical modeling suggests that necking depends on pre-rift lithosphere thickness as well, with thinner lithospheres producing narrower rifts and rifted margins (e.g., Svartman Dias et al., 2015). It is possible that, in the study area, where the CAR and EAR overlapped, the lithosphere was not fully thermally recovered from the CAR thinning when the EAR thinning occurred, about only 30–40 My later (Figure 3).

### 5.3. Spatial Variations of Thinning Processes

Our observations also illustrate the variability of the deformation processes (e.g., brittle vs. ductile deformation partitioning, ODNF vs. CCDNF, mantle highs) along the Guiana Shield margin.

In the GS basin, the offsets of the CDNF along the divergent segment cannot account for the amount of crustal thinning suggested by the Moho upwelling (Figure 4a). Those faults are rooted in the lower crust that shows evidences for pervasive ductile shearing (Figure 4). Following Clerc et al. (2015), these features would suggest top-to-the-east sense of shear, synthetic to the normal faults (Figure 4a). A significant part of the thinning was therefore most likely achieved by lower crustal ductile deformation, which would be typical of volcanic or hot passive margins as proposed by Clerc et al. (2018). Underplating features in the

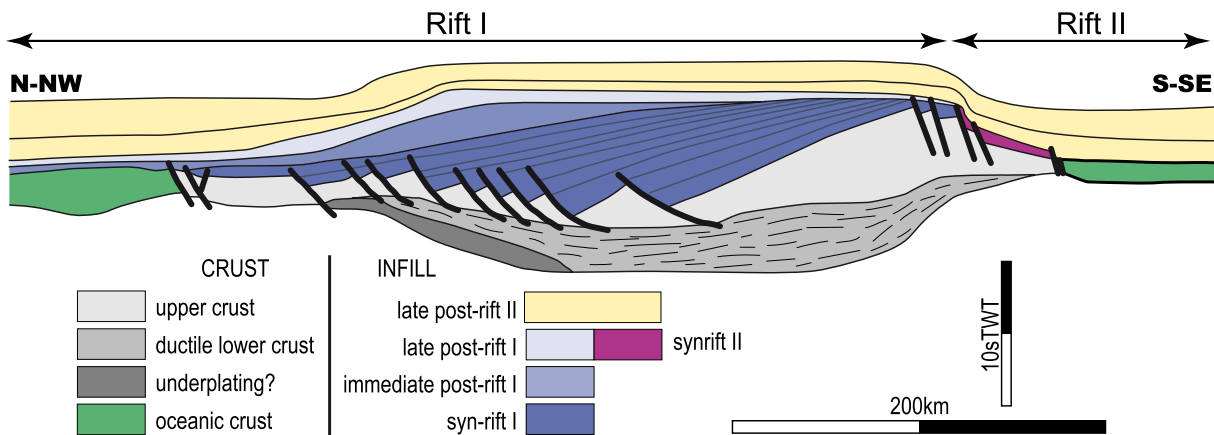


**Figure 11.** Schematic cross-section across the Demerara Plateau continental block illustrating the difference in necking style and thinning processes between the CAR (Rift I) and the EAR (Rift II).

necking domain and the fact that oceanic crust is thicker than average (>12 km; e.g., Reuber et al., 2016; Figure 4a) are consistent as well with this type of “hot” margins. Besides, the suggestion that the syn-rift deposits are volcanic would imply that it is a volcanic margin (Museum et al., 2020; Nemčok et al., 2016; Reuber et al., 2016). Nevertheless, evidence for a hot or volcanic margin is not attested along the neighboring T1 and O1 segments. Furthermore, shear sense in the lower crust cannot be readily determined along those segments (Figures 4b and 4c). Finally, along T1 and O1 segments, the syn-rift deposits are less voluminous and show no indications of SDR. Partitioning between brittle and ductile deformation is nonetheless probable along these segments as well to account for the crustal thinning, given the limited deformation apparently accommodated by normal faults (Figures 4b and 4c).

In the Equatorial Atlantic domain (where thinning results from the Cretaceous EAR, i.e., from segments T2 to O3), the crustal thinning processes appear to be different from those documented in the GS basin. The lower crust shows fewer shear deformation features (Figure 6). Syn-rift deposits are less voluminous, show no SDR and are mostly clastics (Figures 5 and 6). Normal faults in the necking and hyper-extended domains alternate laterally from CDFN to ODNF, suggesting variable conjugate shear patterns in the lower crust along the margin (Figures 6, 8 and 9). The oceanic crust is thinner than average (Figures 6 and 8). Overall, this suggests that the Equatorial Atlantic rifting affected a colder lithosphere than the Central Atlantic rifting, in agreement with an influence of the CAMP and Sierra Leone hotspot on Jurassic rifting processes (e.g., Basile et al., 2020; Marzoli et al., 1999; Nomade et al., 2007).

#### 5.4. The Demerara Plateau: Continental Relic of a Rift Junction

Our results illustrate how the two-step crustal thinning of the Demerara Plateau (at the junction of the CAR and EAR) produced a peculiar crustal structure over a limited (500 × 250 km) area (Figures 4a, 8, 9 and 11). To the NW, the necking and distal margin domains are very wide (>300 km). Thinning was accommodated by a significant component ductile deformation and allowed for the preservation of a thick volcano-clastic syn-rift in-fill (Figures 4a and 11). To the SE, the necking and hyper-extended domains are much narrower (120 km), with limited indication of ductile deformation and a reduced syn-rift clastic infill (Figures 4a and 11). Finally, to the N, the margin has a very narrow necking domain (20–25 km) and no hyper-extended domain or indication of ductile deformation and received a very reduced syn-rift clastic infill (Figure 5).

We show that the Demerara Plateau has evolved from a Jurassic rift to an isolated promontory of continental crust after separation of the South American and African continental lithospheres (Figures 7d and 11). Above the CABU, the thin post-rift sedimentary wedge on top of the Demerara Plateau indicates that this crustal domain underwent less subsidence than the surrounding margin segments and oceanic domains (Figures 4, 5 and 11). Indeed, crustal thinning was compensated by the thick syn-rift Jurassic deposits that make up to more than one third of the present-day crustal thickness of the Demerara Plateau (Figures 4 and 11). This allowed for that crustal domain to remain relatively thick and therefore high with respect to the adjoining margin

segments and oceanic domains because of isostasy. If the D1 divergent segment was magmatic, underplating might have further contributed to the plateau crustal thickness and relative height (Figures 4, 5 and 11).

Isolation of the Demerara Plateau resulted from the interaction of two diachronous rift systems (Figure 11). We suggest that the Demerara Plateau example illustrates a tectonic mechanism able to produce continental ribbons, blocks or promontories at obliquely divergent continental margins with complex map traces, as opposed to more rectilinear divergent margins. The 3D crustal geometry of Demerara-type continental blocks would have a first-order impact on the inversion mode of such continental margin under convergence in collisional orogens.

## 6. Conclusions

1. This work documented the development of the Guiana shield passive margin at the junction of the Central (Jurassic) and Equatorial (Cretaceous) Atlantic rifts by mapping the crustal and sedimentary structure of the Guiana-Suriname basin, Demerara plateau and Foz do Amazonas basin.
2. The contrasted kinematics of the two rifts (southern tip of the Central Atlantic rift vs. oblique en-échelon Equatorial Atlantic rift) and their superimposition produced a complex margin with alternating transform, oblique and divergent margin segments, typically.
3. The width of the margin segments is variable, with narrower transform/oblique segments and wider divergent segments. The transform segments do not include an hyperextended or a distal margin domains, further amplifying the width difference. Thus, the higher the obliquity to the extension direction, the narrower the margin segments.
4. Equatorial Atlantic rifting produced generally narrower segments than Central Atlantic rifting. This is primarily due to the higher obliquity and rates of the Equatorial Atlantic rifting with respect to the Central Atlantic rifting
5. Along the western border of the Demerara plateau, Central Atlantic rifting produced wide (>300 km) necking and distal margin domains, pervasive lower crustal ductile deformation, a thick volcano-clastic syn-rift in-fill, potential underplating and a thicker than average oceanic crust. By contrast, Equatorial Atlantic rifting produced narrower necking and hyper-extended domains (100–150 km), limited lower crustal ductile deformation, reduced syn-rift clastic infill and thinner than average oceanic crust. This suggests that Equatorial Atlantic rifting affected a colder lithosphere than Central Atlantic rifting.
6. The continental lithosphere of the Demerara Plateau, where the two rifts overlapped, was therefore thinned twice. The plateau became however an isolated buoyant continental promontory because its crust consists mostly of very thick Jurassic volcano-sedimentary syn-rift deposits.

## Data Availability Statement

Part of the sub-surface data used for this research is shown in Museur et al., 2020, Nemčok et al. (2016), Sapin et al. (2016) and Reuber et al. (2016).

## Acknowledgments

The authors thank the Bureau de Recherches Géologiques et Minières and Total for funding this work within the framework of the S2S project and the R&D Total group for providing subsurface data. The authors thank P. Angrand, N. Belhassen and Y. Denèle for discussions. Sub-surface data are under restrictive proprietary license and thus not open for distribution. The authors thank C. Basile, K. Reuber and an anonymous reviewer for their thorough reviews and suggestions for manuscript improvement.

## References

- Antobreh, A. A., Faleide, J. I., Tsikalas, F., & Planke, S. (2009). Rift-shear architecture and tectonic development of the Ghana margin deduced from multichannel seismic reflection and potential field data. *Marine and Petroleum Geology*, 26(3), 345–368. <https://doi.org/10.1016/j.marpetgeo.2008.04.005>
- Attoh, K., Brown, L., Guo, J., & Heanlein, J. (2004). Seismic stratigraphic record of transpression and uplift on the Romanche transform margin, offshore Ghana. *Tectonophysics*, 378(1–2), 1–16. <https://doi.org/10.1016/j.tecto.2003.09.026>
- Autin, J., Bellahsen, N., Leroy, S., Husson, L., Beslier, M.-O., & d'Acremont, E. (2013). The role of structural inheritance in oblique rifting: Insights from analogue models and application to the Gulf of Aden. *Tectonophysics*, 607, 51–64. <https://doi.org/10.1016/j.tecto.2013.05.041>
- Basile, C. (2015). Transform continental margins—Part 1: Concepts and models. *Tectonophysics*, 661, 1–10. <https://doi.org/10.1016/j.tecto.2015.08.034>
- Basile, C., Girault, I., Paquette, J. L., Agranier, A. M., Loncke, L., Heuret, A., & Poetisi, E. (2020). The Jurassic magmatism of the Demerara Plateau (offshore French Guiana) as a remnant of the Sierra Leone hotspot during the Atlantic rifting. *Scientific Reports*, 10, 7486. <https://doi.org/10.1038/s41598-020-64333-5>
- Basile, C., Maillard, A., Patriat, M., Gaullier, V., Loncke, L., Roest, W., et al. (2013). Structure and evolution of the Demerara Plateau, offshore French Guiana: Rifting, tectonic inversion and post-rift tilting at transform-divergent margins intersection. *Tectonophysics*, 591, 16–29. <https://doi.org/10.1016/j.tecto.2012.01.010>

- Basile, C., Mascle, J., Benkheil, J., & Bouillin, J. P. (1998). Geodynamic evolution of the Ivory Coast-Ghana transform margin: An overview from Leg 159 results. *Proceedings of the Ocean Drilling Program, Scientific Results*, 15, 101–110.
- Basile, C., Mascle, J., & Guiraud, R. (2005). Phanerozoic geological evolution of the Equatorial Atlantic domain. *Journal of African Earth Sciences*, 43(1–3), 275–282. <https://doi.org/10.1016/j.jafrearsci.2005.07.011>
- Bellahsen, N., Leroy, S., Autin, J., Razin, P., d'Acremont, E., Sloan, H., et al. (2013). Pre-existing oblique transfer zones and transfer/transform relationships in continental margins: New insights from the southeastern Gulf of Aden, Socotra Island, Yemen. *Tectonophysics*, 607, 32–50.
- Benkheil, J., Mascle, J., & Tricart, P. (1995). The Guinea continental margin: An example of a structurally complex transform margin. *Tectonophysics*, 248(1–2), 117–137. [https://doi.org/10.1016/0040-1951\(94\)00246-6](https://doi.org/10.1016/0040-1951(94)00246-6)
- Bennett, K. C., & Rusk, D. (2002). Regional 2D seismic interpretation and exploration potential of offshore deepwater Sierra Leone and Liberia, West Africa. *The Leading Edge*, 21(11), 1118–1124. <https://doi.org/10.1190/1.1523743>
- Brandão, J., & Feijó, F. (1994). Bacia da foz do Amazonas. *Boletim de Geociências da Petrobras*, 8(1), 91–99.
- Brune, S. (2014). Evolution of stress and fault patterns in oblique rift systems: 3-D numerical lithospheric-scale experiments from rift to breakup. *Geochemistry, Geophysics, Geosystems*, 15(8), 3392–3415. <https://doi.org/10.1002/2014GC005446>
- Brune, S., Popov, A. A., & Sobolev, S. V. (2012). Modeling suggests that oblique extension facilitates rifting and continental break-up. *Journal of Geophysical Research*, 117(B8), B08402. <https://doi.org/10.1029/2011JB008860>
- Brune, S., Williams, S. E., Butterworth, N. P., & Müller, R. D. (2016). Abrupt plate accelerations shape rifted continental margins. *Nature*, 536(7615), 201–204. <https://doi.org/10.1038/nature18319>
- Brune, S., Williams, S. E., & Müller, R. D. (2018). Oblique rifting: The rule, not the exception. *Solid Earth*, 9(5), 1187–1206. <https://doi.org/10.5194/se-9-1187-2018>
- Buck, W. R. (1991). Modes of continental lithospheric extension. *Journal of Geophysical Research*, 96(B12), 20161–20178. <https://doi.org/10.1029/91JB01485>
- Campan, A. (1995). *Analyse cinématique de l'Atlantique Equatorial: Implication sur l'évolution de l'Atlantique Sud et sur la frontière de l'Amérique du Nord/Amérique du Sud (Doctoral Dissertation)*. Paris: Université Pierre et Marie Curie.
- Clerc, C., Jolivet, L., & Ringenbach, J.-C. (2015). Ductile extensional shear zones in the lower crust of a passive margin. *Earth and Planetary Science Letters*, 431, 1–7. <https://doi.org/10.1016/j.epsl.2015.08.038>
- Clerc, C., Ringenbach, J.-C., Jolivet, L., & Ballard, J.-F. (2018). Rifted margins: Ductile deformation, boudinage, continentward-dipping normal faults and the role of the weak lower crust. *Gondwana Research*, 53, 20–40. <https://doi.org/10.1016/j.gr.2017.04.030>
- Clifton, A. E., Schlische, R. W., Withjack, M. O., & Ackermann, R. V. (2000). Influence of rift obliquity on fault-population systematics: Results of experimental clay models. *Journal of Structural Geology*, 22(10), 1491–1509. [https://doi.org/10.1016/S0191-8141\(00\)00043-2](https://doi.org/10.1016/S0191-8141(00)00043-2)
- Cordani, U. G., Ramos, V. A., Fraga, L. M., Cegarra, M., Delgado, I., de Souza, K. G., et al. (2016). *Tectonic map of south America (scale 1:5,000,000)*. Paris: CGMW-CPRM-SEGEMAR.
- Costa, J. B. S., Hasui, Y., Bemerguy, R. L., Soares-Júnior, A. V., & Villegas, J. M. C. (2002). Tectonics and paleogeography of the Marajó basin, northern Brazil. *Anais Da Academia Brasileira de Ciências*, 74(3), 519–531. <https://doi.org/10.1590/S0001-37652002000300013>
- Crawford, F. D., Szelewski, C. E., & Alvey, G. D. (1985). Geology and exploration in the Takutu graben of Guyana and Brazil. *Journal of Petroleum Geology*, 8(1), 5–36. <https://doi.org/10.1111/j.1747-5457.1985.tb00189.x>
- Davison, I., Faull, T., Greenhalgh, J., Beirne, E. O., & Steel, I. (2016). Transpressional structures and hydrocarbon potential along the Romanche Fracture Zone: A review. *Geological Society, London, Special Publications*, 431(1), 235–248. <https://doi.org/10.1144/SP431.2>
- Destro, N., Szatmari, P., & Ladeira, E. A. (1994). Post-Devonian transpressional reactivation of a Proterozoic ductile shear zone in Ceará, NE Brazil. *Journal of Structural Geology*, 16(1), 35–45. [https://doi.org/10.1016/0191-8141\(94\)90016-7](https://doi.org/10.1016/0191-8141(94)90016-7)
- Duclaux, G., Huismans, R., & May, D. (2020). Rotation, narrowing, and preferential reactivation of brittle structures during oblique rifting. *Earth and Planetary Science Letters*, 531, 115952. <https://doi.org/10.1016/j.epsl.2019.115952>
- Fairhead, J. D. (1988). Mesozoic plate tectonic reconstructions of the central South Atlantic Ocean: The role of West and Central African rift system. *Tectonophysics*, 155, 181–191. [https://doi.org/10.1016/0040-1951\(88\)90265-x](https://doi.org/10.1016/0040-1951(88)90265-x)
- Figueiredo, J. P., Zalán, P. V., & Soares, E. F. (2007). Bacia da Foz do Amazonas. *Boletim de Geociências da Petrobras*, 15, 299–309.
- Frizon de Lamotte, D. F., Fourdan, B., Leleu, S., Leparmentier, F., & de Clarens, P. (2015). Style of rifting and the stages of Pangea breakup. *Tectonics*, 34, 1009–1029. <https://doi.org/10.1002/2014TC003760>
- Genik, G. J. (1992). Regional framework, structural and petroleum aspects of rift basins in Niger, Chad and the Central African Republic (C.A.R.). *Tectonophysics*, 213, 169–185. <https://doi.org/10.1016/b978-0-444-89912-5.50036-3>
- Gillard, M., Sauter, D., Tugend, J., Tomasi, S., Epin, M.-E., & Manatschal, G. (2017). Birth of an oceanic spreading center at a magma-poor rift system. *Scientific Reports*, 7(1), 15072. <https://doi.org/10.1038/s41598-017-15522-2>
- Greenroyd, C. J., Peirce, C., Rodger, M., Watts, A. B., & Hobbs, R. W. (2007). Crustal structure of the French Guiana margin, West Equatorial Atlantic. *Geophysical Journal International*, 169(3), 964–987. <https://doi.org/10.1111/j.1365-246X.2007.03372.x>
- Greenroyd, C. J., Peirce, C., Rodger, M., Watts, A. B., & Hobbs, R. W. (2008). Do fracture zones define continental margin segmentation?—Evidence from the French Guiana margin. *Earth and Planetary Science Letters*, 272(3–4), 553–566. <https://doi.org/10.1016/j.epsl.2008.05.022>
- Guiraud, M. (1993). Late Jurassic rifting—Early Cretaceous rifting and late Cretaceous transpressional inversion in the upper Benue basin (NE Nigeria). *Bulletin des Centres de Recherche Exploration-Production Elf Aquitaine*, 17(2), 371–383.
- Guiraud, R., Binks, R., Fairhead, J., & Wilson, M. (1992). Chronology and geodynamic setting of Cretaceous Cenozoic rifting in West and Central Africa. *Tectonophysics*, 213(1–2), 227–234. [https://doi.org/10.1016/0040-1951\(92\)90260-D](https://doi.org/10.1016/0040-1951(92)90260-D)
- Heine, C., Zoethout, J., & Müller, R. D. (2013). Kinematics of the South Atlantic rift. *Solid Earth*, 4(2), 215–253. <https://doi.org/10.5194/se-4-215-2013>
- Hoorn, C., Guerrero, J., Sarmiento, G. A., & Lorente, M. A. (1995). Andean tectonics as a cause for changing drainage patterns in Miocene northern South America. *Geology*, 23(3), 237. [https://doi.org/10.1130/0091-7613\(1995\)023<0237:ATAACF>2.3.CO;2](https://doi.org/10.1130/0091-7613(1995)023<0237:ATAACF>2.3.CO;2)
- Hoorn, C., Wesselingh, F. P., ter Steege, H., Bermudez, M. A., Mora, A., Sevink, J., et al. (2010). Amazonia through time: Andean uplift, climate change, landscape evolution, and biodiversity. *Science*, 330(6006), 927–931. <https://doi.org/10.1126/science.1194585>
- Jeannot, L., & Buitert, S. J. H. (2018). A quantitative analysis of transtensional margin width. *Earth and Planetary Science Letters*, 491, 95–108. <https://doi.org/10.1016/j.epsl.2018.03.003>
- Klitgord, K., & Schouten, H. (1986). Plate kinematics of the Central Atlantic. In P. R. Vogt & B. E. Tucholke (Eds.), *The geology of North America, vol. M, the western North Atlantic region* (pp. 351–378). Boulder, CO: Geological Society of America.
- Kusznir, N. J., Roberts, A. M., & Alvey, A. D. (2018). Crustal structure of the conjugate Equatorial Atlantic Margins, derived by gravity anomaly inversion. *Geological Society, London, Special Publications*, 476, 476–107. <https://doi.org/10.1144/SP476.5>

- Labails, C., Olivet, J.-L., Aslanian, D., & Roest, W. R. (2010). An alternative early opening scenario for the Central Atlantic Ocean. *Earth and Planetary Science Letters*, 297(3–4), 355–368. <https://doi.org/10.1016/j.epsl.2010.06.024>
- Loncke, L., Droz, L., Gaullier, V., Basile, C., Patriat, M., & Roest, W. (2009). Slope instabilities from echo-character mapping along the French Guiana transform margin and Demerara abyssal plain. *Marine and Petroleum Geology*, 26(5), 711–723. <https://doi.org/10.1016/j.marpetgeo.2008.02.010>
- Loncke, L., Maillard, A., Basile, C., Roest, W. R., Bayon, G., Gaullier, V., et al. (2016). Structure of the Demerara passive-transform margin and associated sedimentary processes. Initial results from the IGUANES cruise. *Geological Society, London, Special Publications*, 431, 179–197. <https://doi.org/10.1144/SP431.7>
- Loncke, L., Roest, W. R., Klingelhoefer, F., Basile, C., Graindorge, D., Heuret, A., et al. (2020). Transform marginal plateaus. *Earth-Science Reviews*, 203, 102940. <https://doi.org/10.1016/j.earscirev.2019.102940>
- Marinho, M., Mascle, J., & Wannesson, J. (1988). Structural framework of the southern Guinean margin (Central Atlantic). *Journal of African Earth Sciences*, 7(2), 401–408. [https://doi.org/10.1016/0899-5362\(88\)90085-1](https://doi.org/10.1016/0899-5362(88)90085-1)
- Marzoli, A., Renne, P. R., Piccirillo, E. M., Ernesto, M., Bellieni, G., & De Min, A. (1999). Extensive 200-million-year-old continental flood basalts of the Central Atlantic magmatic province. *Science*, 284(5414), 616–618. <https://doi.org/10.1126/science.284.5414.616>
- Mascle, J., & Blarez, E. (1987). Evidence for transform margin evolution from the Ivory Coast-Ghana continental margin. *Nature*, 326(6111), 378–381. <https://doi.org/10.1038/326378a0>
- Mascle, J., Blarez, E., & Marinho, M. (1988). The shallow structures of the Guinea and Ivory Coast-Ghana transform margins: Their bearing on the Equatorial Atlantic Mesozoic evolution. *Tectonophysics*, 155(1–4), 193–209. [https://doi.org/10.1016/0040-1951\(88\)90266-1](https://doi.org/10.1016/0040-1951(88)90266-1)
- McConnell, R. (1969). Notes and discussions, fundamental fault zones in the Guiana and West African shields in relation to presumed axes of Atlantic spreading. *The Geological Society of America Bulletin*, 80(9), 1775–1782. [https://doi.org/10.1130/0016-7606\(1969\)80\[1775:nadffz\]2.0.co;2](https://doi.org/10.1130/0016-7606(1969)80[1775:nadffz]2.0.co;2)
- Mercier de Lépinay, M. (2016). *Inventaire mondial des marges transformantes et évolution tectono-sédimentaire des plateaux de Demerara et de Guinée (Doctoral dissertation)*. Perpignan: Université de Perpignan.
- Mercier de Lépinay, M., Loncke, L., Basile, C., Roest, W. R., Patriat, M., Maillard, A., & De Clarens, P. (2016). Transform continental margins—Part 2: A worldwide review. *Tectonophysics*, 693, 96–115. <https://doi.org/10.1016/j.tecto.2016.05.038>
- Merdith, A. S., Williams, S. E., Brune, S., Collins, A. S., & Müller, R. D. (2019). Rift and plate boundary evolution across two supercontinent cycles. *Global and Planetary Change*, 173, 1–14. <https://doi.org/10.1016/j.gloplacha.2018.11.006>
- Milani, E. J., Rangel, H. D., Bueno, G. V., Stica, J. M., Winter, W. R., Caixeta, J. M., & Neto, O. P. (2007). Bacias sedimentares brasileiras: Cartas estratigráficas. *Anexo Ao Boletim de Geociências Da Petrobrás*, 15(1), 183–205.
- Morley, C. K., Wescott, W. A., Stone, D. M., Harper, R. M., Wigger, S. T., & Karanja, F. M. (1992). Tectonic evolution of the northern Kenyan Rift. *Journal of the Geological Society*, 149(3), 333–348. <https://doi.org/10.1144/gsjgs.149.3.0333>
- Moulin, M., Aslanian, D., & Unternehr, P. (2010). A new starting point for the South and Equatorial Atlantic Ocean. *Earth-Science Reviews*, 98(1–2), 1–37. <https://doi.org/10.1016/j.earscirev.2009.08.001>
- Moullade, M., Mascle, J., Benkheilil, J., Cousin, M., & Tricart, P. (1993). Occurrence of marine mid-Cretaceous sediments along the Guinean slope (Equamarge II cruise): Their significance for the evolution of the Central Atlantic African margin. *Marine Geology*, 110(1–2), 63–72. [https://doi.org/10.1016/0025-3227\(93\)90105-5](https://doi.org/10.1016/0025-3227(93)90105-5)
- Museur, T., Graindorge, D., Klingelhoefer, F., Roest, W. R., Basile, C., Loncke, L., & Sapin, F. (2020). Deep structure of the Demerara Plateau: From a volcanic margin to a Transform Marginal Plateau. *Tectonophysics*, 803, 228645. <https://doi.org/10.1016/j.tecto.2020.228645>
- Nemčok, M., Rybár, S., Odegard, M., Dickson, W., Pelech, O., Ledvényiová, L., et al. (2016). Development history of the southern terminus of the Central Atlantic; Guyana-Suriname case study. *Geological Society, London, Special Publications*, 431, 145–178. <https://doi.org/10.1144/SP431.10>
- NOAA National Geophysical Data Center (2009). *ETOPO1 1 arc-minute global relief model*. NOAA National Centers for Environmental Information. <https://doi.org/10.7289/V5C8276M>
- Nomade, S., Knight, K. B., Beutel, E., Renne, P. R., Verati, C., Féraud, G., et al. (2007). Chronology of the Central Atlantic Magmatic Province: Implications for the Central Atlantic rifting processes and the Triassic-Jurassic biotic crisis. *Palaeogeography, Palaeoclimatology, Palaeoecology*, 244(1–4), 326–344. <https://doi.org/10.1016/j.palaeo.2006.06.034>
- Olyphant, J. R., Johnson, R. A., & Hughes, A. N. (2017). Evolution of the Southern Guinea Plateau: Implications on Guinea-Demerara Plateau formation using insights from seismic, subsidence, and gravity data. *Tectonophysics*, 717, 358–371. <https://doi.org/10.1016/j.tecto.2017.08.036>
- Peron-Pinvidic, G., Manatschal, G., & Osmundsen, P. T. (2013). Structural comparison of archetypal Atlantic rifted margins: A review of observations and concepts. *Marine and Petroleum Geology*, 43, 21–47. <https://doi.org/10.1016/j.marpetgeo.2013.02.002>
- Pindell, J. L. (1985). Alleghenian reconstruction and subsequent evolution of the Gulf of Mexico, Bahamas, and Proto-Caribbean. *Tectonics*, 4(1), 1–39. <https://doi.org/10.1029/TC004i001p00001>
- Pindell, J. L., & Kennan, L. (2009). Tectonic evolution of the Gulf of Mexico, Caribbean and northern South America in the mantle reference frame: An update. *Geological Society, London, Special Publications*, 328(1), 1–55. <https://doi.org/10.1144/SP328.1>
- Planke, S., Symonds, P. A., Alvestad, E., & Skogseid, J. (2000). Seismic volcanostratigraphy of large-volume basaltic extrusive complexes on rifted margins. *Journal of Geophysical Research*, 105(B8), 19335–19351. <https://doi.org/10.1029/1999JB900005>
- Rabinowitz, P. D., & LaBrecque, J. (1979). The Mesozoic South Atlantic Ocean and evolution of its continental margins. *Journal of Geophysical Research*, 84(B11), 5973. <https://doi.org/10.1029/JB084iB11p05973>
- Reuber, K. R., Pindell, J., & Horn, B. W. (2016). Demerara Rise, offshore Suriname: Magma-rich segment of the Central Atlantic Ocean, and conjugate to the Bahamas hot spot. *Interpretation*, 4(2), T141–T155. <https://doi.org/10.1190/INT-2014-0246.1>
- Rodger, M., Watts, A. B., Greenroyd, C. J., Peirce, C., & Hobbs, R. W. (2006). Evidence for unusually thin oceanic crust and strong mantle beneath the Amazon Fan. *Geology*, 34(12), 1081. <https://doi.org/10.1130/G22966A.1>
- Sapin, F., Davaux, M., Dall'asta, M., Lahmi, M., Baudot, G., & Ringenbach, J.-C. (2016). Post-rift subsidence of the French Guiana hyper-oblique margin: From rift-inherited subsidence to Amazon deposition effect. *Geological Society, London, Special Publications*, 431, 125–144. <https://doi.org/10.1144/SP431.11>
- Scarselli, N., Duval, G., Martin, J., McClay, K., & Toothill, S. (2018). Insights into the early evolution of the Côte d'Ivoire Margin (West Africa). *Geological Society, London, Special Publications*, 476, 109–133. <https://doi.org/10.1144/SP476.8>
- Schettino, A., & Turco, E. (2009). Breakup of Pangaea and plate kinematics of the Central Atlantic and Atlas regions. *Geophysical Journal International*, 178(2), 1078–1097. <https://doi.org/10.1111/j.1365-246X.2009.04186.x>
- Schiffer, C., Doré, A. G., Foulger, G. R., Franke, D., Geoffroy, L., Gernigon, L., et al. (2020). Structural inheritance in the North Atlantic. *Earth-Science Reviews*, 206, 102975. <https://doi.org/10.1016/j.earscirev.2019.102975>

- Shephard, G. E., Müller, R. D., Liu, L., & Gurnis, M. (2010). Miocene drainage reversal of the Amazon River driven by plate-mantle interaction. *Nature Geoscience*, 3(12), 870–875. <https://doi.org/10.1038/ngeo1017>
- Staatsolie (2013). *Suriname: The E&P landscape. A brief overview of the petroleum geology in Suriname*. Paramaribo: Staatsolie. Retrieved from <http://www.staatsolie.com>
- Stampfli, G. M., & Borel, G. D. (2002). A plate tectonic model for the Paleozoic and Mesozoic constrained by dynamic plate boundaries and restored synthetic oceanic isochrons. *Earth and Planetary Science Letters*, 196(1–2), 17–33. [https://doi.org/10.1016/S0012-821X\(01\)00588-X](https://doi.org/10.1016/S0012-821X(01)00588-X)
- Stanton, N., Kuszniir, N., Gordon, A., & Schmitt, R. (2019). Architecture and Tectono-magmatic evolution of the Campos Rifted Margin: Control of OCT structure by basement inheritance. *Marine and Petroleum Geology*, 100, 43–59. <https://doi.org/10.1016/j.marpetgeo.2018.10.043>
- Sutra, E., Manatschal, G., Mohn, G., & Unternehr, P. (2013). Quantification and restoration of extensional deformation along the Western Iberia and Newfoundland rifted margins: Strain distribution along rifted margins. *Geochemistry, Geophysics, Geosystems*, 14(8), 2575–2597. <https://doi.org/10.1002/ggge.20135>
- Svartman Dias, A. E., Lavier, L. L., & Hayman, N. W. (2015). Conjugate rifted margins width and asymmetry: The interplay between lithospheric strength and thermomechanical processes. *Journal of Geophysical Research: Solid Earth*, 120(12), 8672–8700. <https://doi.org/10.1002/2015JB012074>
- Szatmari, P. (1983). Amazon rift and Pisco-Jurua fault: Their relation to the separation of North America from Gondwana. *Geology*, 11(5), 300–304. [https://doi.org/10.1130/0091-7613\(1983\)11<300:ARAPFT>2.0.CO;2](https://doi.org/10.1130/0091-7613(1983)11<300:ARAPFT>2.0.CO;2)
- Tetreault, J. L., & Buijter, S. J. H. (2018). The influence of extension rate and crustal rheology on the evolution of passive margins from rifting to break-up. *Tectonophysics*, 746, 155–172. <https://doi.org/10.1016/j.tecto.2017.08.029>
- Tron, V., & Brun, J.-P. (1991). Experiments on oblique rifting in brittle-ductile systems. *Tectonophysics*, 188, 71–84. [https://doi.org/10.1016/0040-1951\(91\)90315-j](https://doi.org/10.1016/0040-1951(91)90315-j)
- vanSoelen, E. E., Kim, J.-H., Santos, R. V., Dantas, E. L., Vasconcelos de Almeida, F., Pires, J. P., et al. (2017). A 30 Ma history of the Amazon River inferred from terrigenous sediments and organic matter on the Ceará Rise. *Earth and Planetary Science Letters*, 474, 40–48. <https://doi.org/10.1016/j.epsl.2017.06.025>
- Versfelt, J., & Rosendahl, B. R. (1989). Relationships between pre-rift structure and rift architecture in Lakes Tanganyika and Malawi, East Africa. *Nature*, 337(6205), 354–357. <https://doi.org/10.1038/337354a0>
- Watts, A. B., Rodger, M., Peirce, C., Greenroyd, C. J., & Hobbs, R. W. (2009). Seismic structure, gravity anomalies, and flexure of the Amazon continental margin, NE Brazil. *Journal of Geophysical Research*, 114(B7), B07103. <https://doi.org/10.1029/2008JB006259>
- Yang, W., & Escalona, A. (2011). Tectonostratigraphic evolution of the Guyana basin. *AAPG Bulletin*, 95(8), 1339–1368. <https://doi.org/10.1306/01031110106>
- Ye, J., Chardon, D., Rouby, D., Guillocheau, F., Dall'asta, M., Ferry, J.-N., & Broucke, O. (2017). Paleogeographic and structural evolution of northwestern Africa and its Atlantic margins since the early Mesozoic. *Geosphere*, 13(4), 1254–1284. <https://doi.org/10.1130/GES01426.1>
- Ye, J., Rouby, D., Chardon, D., Dall'asta, M., Guillocheau, F., Robin, C., & Ferry, J. N. (2019). Post-rift stratigraphic architectures along the African margin of the Equatorial Atlantic: Part I. The influence of extension obliquity. *Tectonophysics*, 753, 49–62. <https://doi.org/10.1016/j.tecto.2019.01.003>
- Zalán, P. V., & Matsuda, N. S. (2007). Bacia do Marajó. *Boletim de Geociências da Petrobras*, 15(2), 311–319.
- Zalán, P. V., Nelson, E. P., Warme, J. E., & Davis, T. L. (1985). *The Piauí basin: Rifting and wrenching in an Equatorial Atlantic transform basin*. SEPM Society for Sedimentary Geology.